Design and Experimental Investigation of a Hydroxyl Ammonium Nitrate Based Workhorse Microthruster

Richard Grist

A thesis

submitted in partial fulfillment of the

requirements for the degree of

Master of Science in Aeronautics and Astronautics

University of Washington

2016

Committee:

Carl Knowlen, Chair

James Hermanson

Program Authorized to Offer Degree:

Aeronautics and Astronautics

University of Washington

Abstract

Design and Experimental Investigation of a
Hydroxyl Ammonium Nitrate Based Workhorse
Microthruster

Richard Grist

Chair of the Supervisory Committee:
Research Associate Professor Carl Knowlen
Aeronautics and Astronautics

Hydroxylammonium nitrate-based (HAN-based) monopropellant is being investigated as an alternative to hydrazine due to its lower inherit hazard of handling and higher energy density. It is hypothesized the light-off temperature and corresponding preheat power required for microthrusters using HAN-based monopropellants decrease with decreasing droplet size. The viscous nature of this propellant, however, creates significant challenges in its atomization. Having developed a means to control the droplet size down to 50 micrometers in diameter, experiments are proceeding with a laboratory-scale workhorse thruster apparatus designed for the operation in the 0.1 - 1 Newton thrust range. As part of this program, the injector atomization capabilities in a pressurized test cell were examined with high speed photography, flow-through light-off experiments were carried out at ambient pressure using interchangeable steel and quartz heated-catalyst housings, and thruster tests were performed at elevated chamber pressures. Results from these experiments show discrepancies between ambient pressure ignition testing of the HAN-based monopropellant and those conducted in the pressure building workhorse thruster. This

may suggest a link between the complete combustion of the propellant and chamber pressure. In the workhorse thruster, successful ignition of the HAN-based monopropellant was obtained with a combustion efficiency of approximately 75 percent.

TABLE OF CONTENTS

LIST OF FIGURES

ACKNOWLEDGEMENTS

First and foremost I would like to thank Dr. Carl Knowlen, my research advisor and principal investigator for the microthruster work conducted at the University of Washington. His guidance and knowledge passed along over the course of this project have proven to be invaluable. I also give my thanks to Dr. Jim Hermanson for sharing his lab space to conduct experiments and being on my master's thesis committee.

I would also like to recognize the NASA Glenn Research Center for sponsoring the research with partnership with Systima Technologies Inc. of whom I appreciate their partnership and cooperation with on the project. From Systima, I would like to give thanks to Gautam Shah and Stephanie Sawhill for all of the time and resources they have invested into the project and for putting up with any of the headaches I may have caused in the process of reviewing papers to be published.

I appreciate fellow graduate research assistant Jeff Glusman for keeping myself sane during the long hours working in the 'grad' room. I would also like to thank undergraduate research associate Greg Derk who has spent countless hours in the research lab running experiments and was instrumental in developing the LabVIEW® script that controls the entire experiment. I also appreciate Charlie Yang for doing all of the random machining work that needed to be done over the course of the project

Lastly, I am grateful for my family who have supported me through my undertakings. They have given me the yearning, willpower, and fortitude to pursue my dreams and have taken the liking of calling me a rocket surgeon.

Chapter 1. INTRODUCTION

Although hydrazine monopropellant has a strong heritage in spacecraft propulsion applications, its toxicity leads to very high costs for shipment, storage, and handling. Green propellants with low toxicity and less inherent hazard have been identified and developed for use in the space industry [1]. In addition to offering greatly reduced handling costs, green monopropellants may provide higher thruster performance than hydrazine propellants, permit shorter launch processing times, and have greater density efficiency that could lead to substantial cost savings and extended mission life for spaceflight missions [2]. Green monopropellants that have been selected for next generation thrusters include HAN-based ionic-salt monopropellants. Green propellants pose several challenges that this new technology seeks to overcome:

1. HAN-based monopropellants are generally more dense and viscous than hydrazine propellant. However, due to viscous effects HAN-based propellants are particularly difficult to accommodate when designing microthrusters, which rely on small flow paths. Traditional propellant-injection technology can achieve atomization but at the cost of high feed pressures with a large injector pressure drop. By finely atomizing the propellant into a uniform spray, it is possible to wet the catalyst bed more evenly than with conventional injector designs to minimize localized erosion caused by high propellant impingement velocity on the catalyst due to the high injection pressure and extend the usable thruster life [3].
2. Current engine designs using HAN-based propellants require a high catalyst bed pre-heat temperature of approximately 300°C to 350°C to initiate propellant ignition and minimize catalyst degradation [4]. Utilizing a finely atomized propellant spray may more efficiently

engage the catalyst. Finer atomization of the monopropellant may promote a greater degree of reaction with the catalyst by increasing the rate of heat transfer and thus decomposition of the HAN-based propellant. This may also allow for lower catalyst bed pre-heat temperatures which results in less heater power required to operate the thruster.

Meeting the challenge of atomizing HAN-based monopropellant to increase thruster performance may stimulate greater utilization of this green propellant in microthruster systems. The ability to generate a fine propellant spray on demand reduces the logistics of generating small impulse bits for precision flying and spacecraft orientation applications. Having developed a very promising technology for droplet atomization, the benefits in terms of reduced input power to catalysts for propellant ignition are being explored. To this end, a workhorse thruster has been designed and fabricated to enable testing of the new injector technology. Light-off characteristics and combustion characteristics will be quantified with this device as function of catalyst initial temperature, catalyst bed length, propellant flow rate, and chamber pressure. The following chapters describe the experimental apparatus used in various subsystem tests carried out and the detailed design of the laboratory scale workhorse thruster. The experimental program had three phases of testing: 1) verification of droplet atomization at high pressure, 2) flow-through ignition tests using heated catalyst without combustion chamber, and 3) workhorse thruster operation over a thrust range of 0.1 – 1 Newton.

Chapter 2. HIGH-PRESSURE ATOMIZATION

2.1 PURPOSE

A pressurized test cell (155 mm-ID x 1000 mm-long) with a pressure rating of 70 bar was used to examine injector operation and atomization quality at the elevated pressures expected during thruster operation. In order to determine operational capability at the expected chamber pressures of the workhorse microthruster system, reliable and complete atomization must first be achieved in a controlled environment.

2.2 DESIGN

A schematic of the pressurized test cell can be seen in Figure 2.1. The design features opposing Vycor® viewing windows with an additional window placed at an angle to illuminate the atomized droplets for high speed photography. The backlit atomized plume was directly imaged using high-speed digital cameras to quantify injector atomization performance. For these experiments the test cell was pressurized up to 20 bar with nitrogen to determine the characteristics of the injector plume atomization at elevated pressures. The appropriate mixture of ethylene-glycol and water was used to simulate the HAN-based monopropellant in these preliminary tests due to its similar density and viscosity properties.

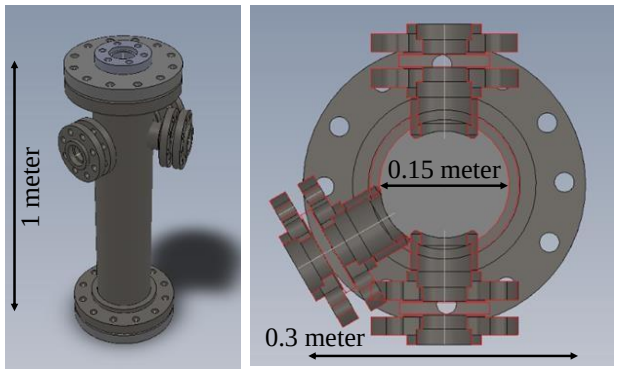

Figure 2.1. **Pressurized test cell for injector studies.**

2.3 TEST RESULTS

Testing was conducted of three custom-built injectors that were developed for use in the workhorse microthruster system and associated testing apparatus. A video frame from a representative injection test using injector number one is seen in Figure 2.2, with a nitrogen backpressure fill of 8.6 bar (125 psia) and a propellant volume flow rate of 10 mL/min. Each atomized fluid particle was subpixel size where one pixel is approximately 200 micrometers in length.

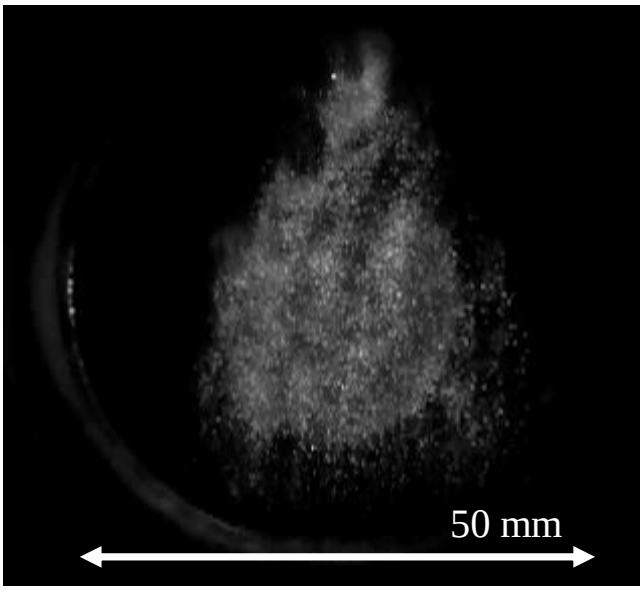

Figure 2.2. **Propellant simulant atomization**

Maximum atomizing flow rate was determined from visual inspection of the plume. Acceptable atomization was characterized as having a uniform flow pattern with no discernable difference in the size of the atomized droplets. Atomization was deemed to be unacceptable when droplets were seen in the plume caused by injector spitting, or when atomization stopped completely and droplets fell from the injector. Figure 2.3 shows a representative still of an atomization test where spitting of the HAN-simulant was seen and a combination of atomized fluid particles and droplets were formed from the injector.

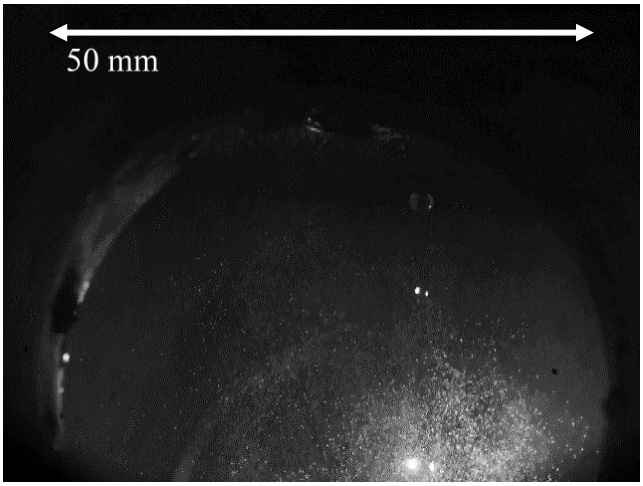

Figure 2.3. **Propellant simulant atomization with large droplet spitting**

The plot in Figure 2.4 shows the maximum flow rate at which three different injector designs were able to atomize the HAN-simulant from ambient up to a nitrogen backfill pressure of 20.7 bar (300 psia). Differences in the injector designs included geometry variations, material construction, and method of mounting the injector. From tests conducted the best performing injector was found to be injector number two. High-pressure testing with injector number two initially produced a maximum flow rate at which atomization can be achieved and maintained to be 34 mL/min at ambient. Between 3.5 to 5 bar (50 - 75 psia), the atomizing flow rate decreased to 28 mL/min, then recovered and leveled off at 32 mL/min flow rate. Even with the small drop in injector performance, the operational margin was deemed adequate for use in the workhorse thruster testing where flow rates up to 20 mL/min and 20 bar were to be expected.

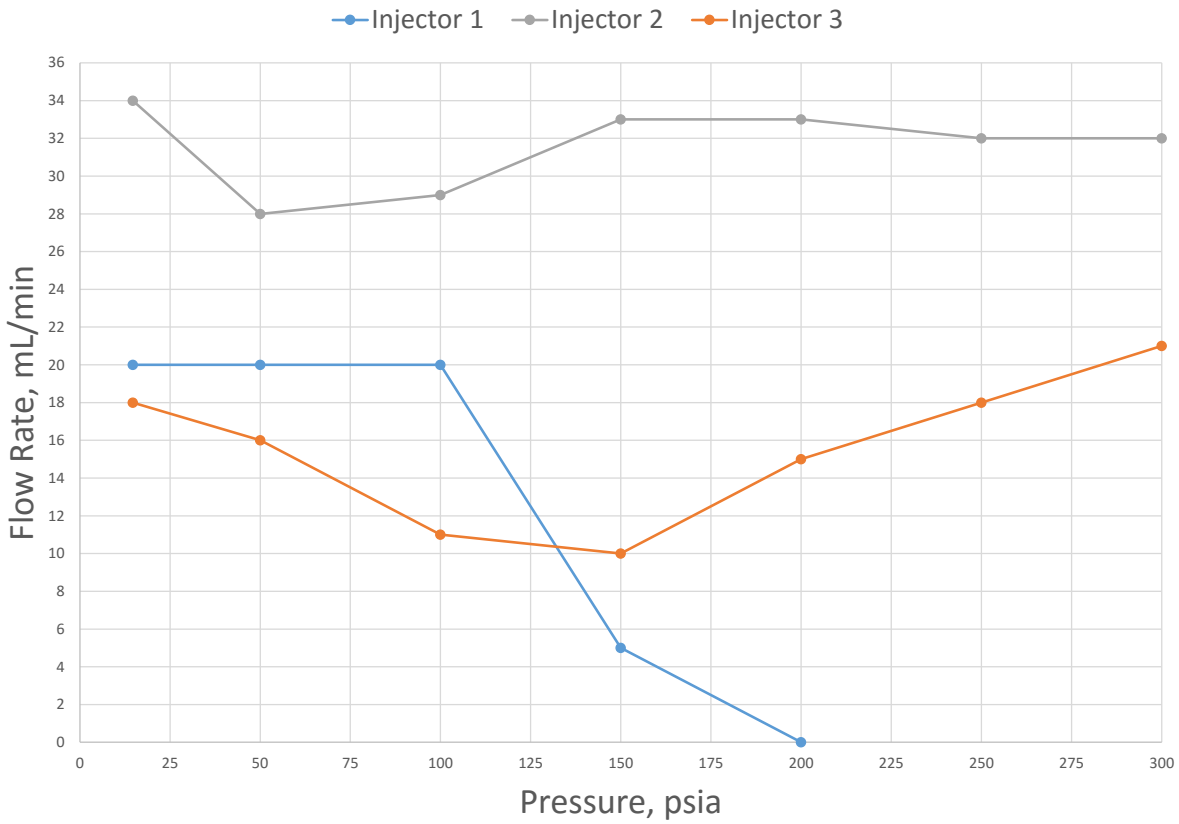

Figure 2.4. **Maximum atomizing flow rate vs. backpressure**

Although injector three was not able to atomize the propellant simulant at as high of a flow rate as injector two for the back pressures tested, injector three showed increased atomization performance as the back pressure increased as determined by visual inspection of the test. The injector initially started with a maximum atomizing flow rate of 18 mL/min at ambient pressure. The injector then passed through a minimum flow rate of 10 mL/min at 10.3 bar (150 psia), the maximum atomizing flow rate then increased to 21 mL/min at the maximum tested pressure of 20.7 bar (300 psia), beyond the maximum atomizing flow rate obtained at ambient pressure.

Injector number one initially showed promise at lower backfill pressures, being able to atomize the HAN simulant at flow rates up to 20 mL/min at fill pressures of 6.9 bar (100 psia). Once the nitrogen backpressure rose above 6.9 bar, injector one showed diminishing results and ceased to atomize the propellant simulant at chamber pressures in excess of 13.8 bar (200 psia). Testing of injector one was not conducted at pressures above 13.8 bar, as such it is unclear whether injector one would show the same trend as injectors two and three and begin to start atomizing once again at a higher chamber pressure. All hot-fire tests have been conducted using injector two due to its reliability and known operational envelope.

Chapter 3. FLOW-THROUGH REACTOR

3.1 PURPOSE

The interaction between the atomized propellant and a heated catalyst bed was examined at ambient pressure through use of a flow-through reactor where atomized propellant was sprayed downward onto the face of a catalyst exposed to an open ambient atmosphere. The metal foam monolithic catalyst used in testing was provided by Plasma Processes, Inc. The propellant ignition characteristics were determined as a function of propellant mass flow rate, catalyst temperature, and catalyst length. Results of these tests helped establish the minimum catalyst length (number of catalysts) needed for microthruster operation. It was anticipated that less catalyst will be required for propellant light-off when the combustor is operated at higher pressurized conditions.

3.2 DESIGN

The flow-through reactor was comprised of three main pieces as seen in Figure 3.1. A two-piece outer stainless steel shell threaded together and housed the temperature instrumentation port for monitoring the catalyst outer surface temperature. The threaded shell was sized to accommodate the dimensions of the electric band heater used during microthruster testing. The other component was an alumina sleeve that was inserted into the stainless steel shell. This served the purpose of minimizing the potential of catalyst poisoning from the back flow of metal oxides that may have formed in the stainless steel combustor

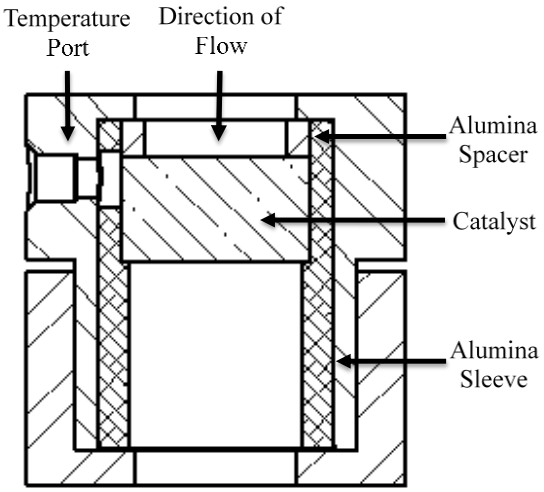

Figure 3.1. **Design of stainless steel flow-through reactor**

during preheat and elevated temperature phases of testing. Once assembled, a clamp attached to a ring stand held the flow-through reactor in place. The injector, which was attached to another stand, was positioned over the flow-through reactor assembly and aligned such that the injector face was approximately 10 millimeters from the top face of the catalyst.

3.3 Test Series and Results

Tests have been performed in the stainless steel flow-through reactor at preheat temperatures of 350°C down to 275°C in 25°C increments at a flow rate of 1 mL/min. Data is shown for this series of tests in Figure 3.2.

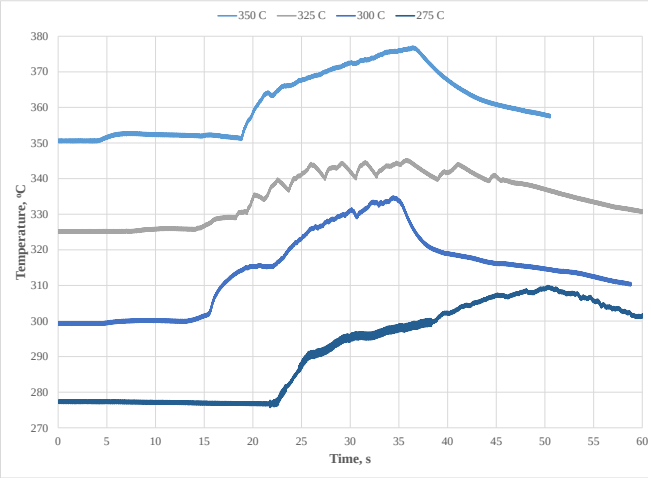

Figure 3.2. **Stainless steel flow-through temperature**

The minimum temperature for light-off of the HAN propellant was found to be 365°C. This was determined in both visual and temperature examination of the flow-through test with a catalyst bed preheat of 350°C. The time-temperature data for this test is the top most data trace in Figure 3.2. For the first 3 seconds of the test after propellant injection started, the flow-through reactor was emitting greyish/white smoke from the propellant interactions with the heated catalyst bed, once the catalyst bed temperature reached 365°C the atomized propellant began to combust on contact with the catalyst bed. In the 325°C test, the second highest temperature trace shown in grey, small air bubbles in the injector line resulted in catalyst temperature pulsations over the course of the run. The end of the propellant injection period corresponds with the drop in catalyst temperature for each test run.

In all runs conducted, a temperature rise was observed in the thermocouple monitoring the outer face of catalyst as the propellant was injected/sprayed onto its top face. For catalyst preheat temperatures below that of the auto-ignition temperature of 365°C, the propellant still underwent an exothermic reaction with the catalyst as seen by the temperature rise in each run. Once the catalyst temperature rose above the minimum ignition temperature, flaring of the propellant occurred as observed through visual examination.

Video recordings were taken of all experiments with a Canon EOS Rebel T4i and GoPro Hero 4 Black. The video frame in Figure 3.3 shows the HAN-based propellant flaring on top of the reactor due to reaction of the propellant with the top surface of the catalyst when the catalyst temperature rose above 365°C. The combustion spreading out over the top of the reactor was caused from the lack of a containment system on the upstream side of the reactor. With ambient air pressure on the upstream and downstream sides of the reactor, the combustion and products advanced in the direction of least resistance which was radially outwards and not through the catalyst bed. The video frame in Figure 3.4 shows fuming at the top surface of the catalyst when the catalyst bed was preheated to 350°C. In this test, much like with that seem in Figure 3.3, there were no

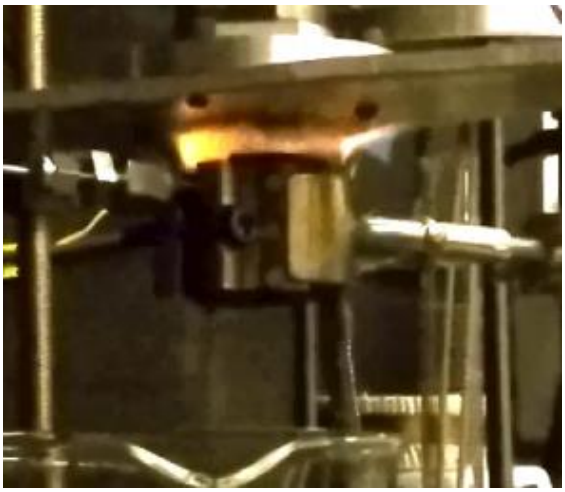

Figure 3.3. **Stainless steel reactor flow-through test, 400°C, 1 mL/min**

Figure 3.4. **Stainless steel reactor flow-through test, 350°C, 1 mL/min**

indications of combustion products passing through the flow-through reactor and catalyst bed. These tests showed that backflow arising from vigorous reactions on the catalyst top surface prevented propellant from flowing through the catalyst in an unpressurized system. In order to obtain useful data in the actual behavior and characteristics of how the monopropellant interacts with and passes through the catalyst bed, a test apparatus that provided a flow path restriction in the region around the upstream area of the catalyst bed was needed.

Chapter 4. VISIBLE FLOW-THROUGH REACTOR

4.1 PURPOSE

To better evaluate the injector performance and HAN-based monopropellant combustion over the catalyst bed, a see-through reactor was manufactured from fused quartz. This combustor allowed visual examination of both the injector spray as it exits the injector and comes into contact with the top face of the catalyst and of the propagation of exothermic reactions as propellant passes through the catalyst. A relatively tight slip-fit between the injector and upstream tube segment of the quartz reactor prevented backflow from escaping at the top of the reactor.

4.2 DESIGN

The test setup for the quartz combustor testing is shown in Figure 4.1. This combustor was fabricated by joining two tubes of fused quartz together, one with an inside diameter of 12.7 millimeters which housed the catalyst bed and another with an inside diameter of 12 millimeters to create a step on which the catalyst bed could rest. The top portion of the quartz combustor created a slip fit seal against the mounting hardware of the injector. By restricting the upwards flow path, combusted products were forced to flow through the catalyst bed and exit out the bottom of the quartz combustor tube. The band heater from the stainless steel flow-through reactor experiments was used with an internal steel sleeve to conduct heat into the catalyst region of the quartz combustor. The quartz combustor flow-through tests were conducted in the same ambient

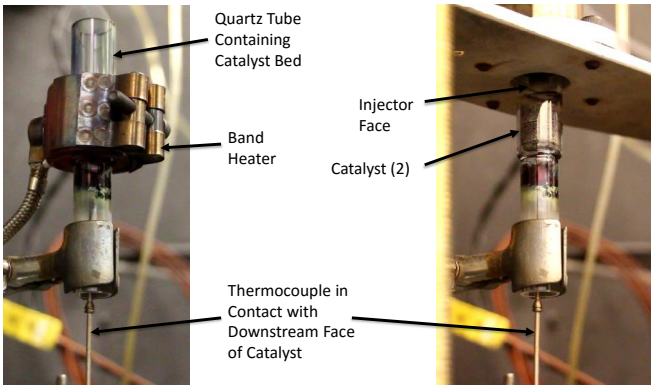

Figure 4.1. **Quartz flow through reactor**

atmosphere environment that the steel flow-through tests were carried out in. If successfully implemented, the flow restriction between the outside of the quartz reactor tube and the injector test stand will build a slight pressure rise upstream of the catalyst bed which will force the reactions to pass through the catalyst bed and exit the quartz reactor on the downstream end.

The preheating process was done without the injector inserted as shown in Figure 4.1 - left. In order to obtain an unobstructed view of the catalyst and the reactions taking place, the band heater was typically removed once the cat-bed temperature had been preheated to 75 to 100°C above the target temperature. The injector stand assembly was then positioned around the quartz combustor, as seen in Figure 4.1 - right, and the cat-bed was allowed to cool until the desired catalyst temperature was reached, as indicated by the Type K thermocouple in contact with the downstream face of the catalyst. The propellant flow was then turned on and the reaction process was observed with video and time-temperature measurements from the thermocouple that remained in contact with the downstream face of the catalyst.

4.3 TEST RESULTS

The quartz combustor test series focused on how catalyst bed length and preheat temperature affected the decomposition of the HAN-based monopropellant. Tests were conducted with one catalyst of length 7.2 millimeters and two catalysts for a total cat-bed length of 14.4 millimeters at propellant flow rates from 1 to 20 mL/min. Pre-heat temperatures ranged from 335 to 450°C.

4.3.1 *Single Catalyst Testing*

For the test shown in Figure 4.2, the catalyst-bed temperature is shown in blue, the start and end of propellant injection are signified by the green and red lines respectively. The catalyst preheat temperature was 360°C, with a propellant flow rate of 2 mL/min for 15 seconds. Due to the nature of the test and the configuration of the apparatus, only the temperature of the downstream face of the catalyst was recorded. It was estimated that due to the limit heat transfer paths, the upstream face of the catalyst was of approximately equal temperature as the downstream face at the start of the test. Visual examination of this test showed the monopropellant initially reacting with the top surface of the catalyst bed and exothermic reactions propagated downward through the catalyst. Furthermore, the representative video frame in Figure 4.2 indicates that the flame front is not uniform as it progressed downward.

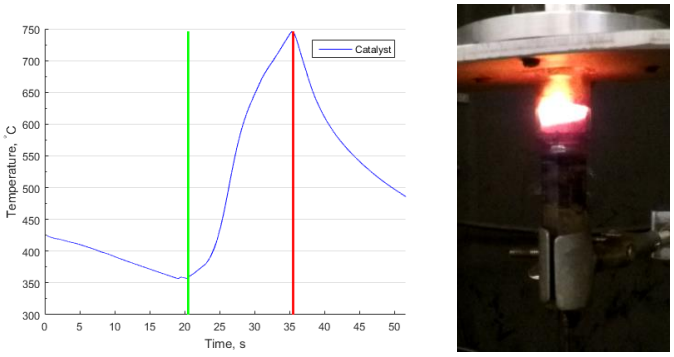

Figure 4.2. **Quartz flow-through test: 2 mL/min**

Tests were conducted up to 20 mL/min in the quartz combustor, this flow rate was the maximum expected flow rate used in the workhorse microthruster. The catalyst time-temperature results are shown in Figure 4.3 along with a representative still taken from the video of the test. The temperature profile of the catalyst-bed showed an immediate spike up to 750°C from a preheat temperature of 400°C.

Figure 4.3. **Quartz flow-through test: 20 mL/min**

After the spike, the thermocouple temperature reading dropped and contained two small prominent temperature spikes, including one that occurred after propellant injection had stopped. The drop in temperature and corresponding spikes were likely caused by unreacted propellant seeping between the outside cylindrical face of the catalyst and the inside of the quartz tube. The unreacted propellant cooled down the exposed thermocouple bead and proceeded to react downstream of the catalyst bed.

As seen in the still frame in Figure 4.3, the flames coming out of the bottom of the quartz reactor were caused by the propellant that was reacting inside the region of the quartz combustor downstream of the catalyst. From video footage of the test the cause for propellant seepage around the catalyst was pooling occurring on the upstream face of the catalyst, this is evident from the dark region on top of the catalyst bed which was the pooled propellant. The pooling on the catalyst was seen on tests at a flow rates of 10 mL/min and greater, it is believed the pooling was caused by the propellant reaction rate with the catalyst not occurring fast enough for the mass flow of incoming propellant to the catalyst activation sites at ambient pressure. Unreacted propellant may pose a risk to the operation of the workhorse microthruster since the possibility of a large amount of propellant reacting simultaneously existed; as a result extra design precautions were considered for the workhorse thruster. Unclear in this test was whether pressure had an effect on the reaction rate of the propellant. In the workhorse microthruster pressure and temperature measurements will be able to determine if a correlation exists.

4.3.2 *Two-Catalyst Testing*

The experimental results from an experiment using two catalysts of the same form factor stacked on top of each other are given in Figure 4.4. This test was conducted at a target preheat temperature of 445°C with a propellant flow rate of 2 mL/min for 15 seconds. The temperature on the lower surface of the bottom catalyst increased by 130°C in the course of this experiment. The propagation of the flame front appeared to be inhibited by the interface between the catalysts, as evident in the video frame shown. Visual examination revealed the upper catalyst was very bright whereas the lower one had a dull red glow. The difference in visual temperature lead to the conclusion that very little to no reactions were taking place in the downstream catalyst. When compared with the test in Figure 4.2, the higher and more uniform temperature observed in the upper catalyst in this test is believed to be caused by flow impedance through the second catalyst bed. The temperature differential between the two catalysts was also enhanced by the thermal contact resistance between the two catalysts. This limited the downward rate of heat conduction and because the surfaces of the catalyst are irregular, the conduction path was limited and can in part explain the large temperature gradient between the two catalysts.

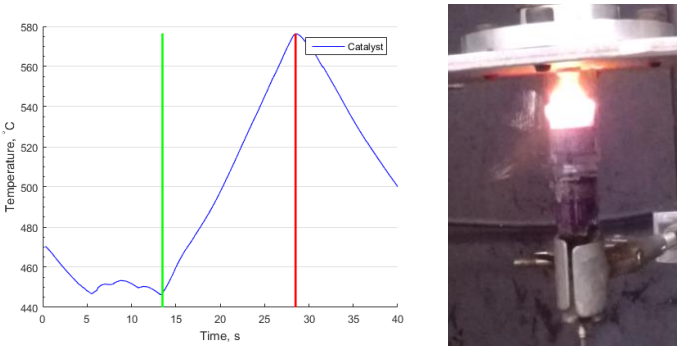

Figure 4.4. **Quartz flow-through test: 2 mL/min**

Increased flow-rate tests with two catalysts showed degraded performance over using a single catalyst. For a test conducted at a flow rate of 15 mL/min, Figure 4.5 shows the catalyst time-temperature response during the test with a corresponding still taken from video of the experiment. The propellant injection began at a catalyst preheat temperature of 400°C and the catalyst temperature spiked to 700°C. However, compared to a similar run at 15 mL/min with a single catalyst, there was significant pooling on the top face of the catalyst bed which was caused by enhanced flow impedance through the longer catalyst bed. The flow impedance through the longer catalyst bed forced the propellant to gather on the top surface and slowly cook off as seen in the extended time the catalyst took to drop in temperature. A possible explanation for the impedance through the catalyst bed was the void volume ratio of the catalysts used is not great enough for the HAN-based propellant to pass through and react without creating a buildup at the higher flow rates of interest.

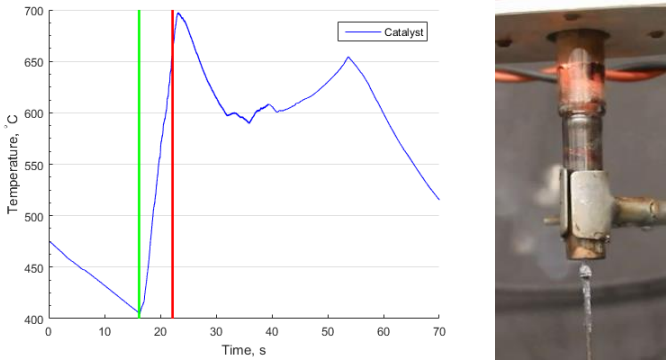

Figure 4.5. **Quartz flow-through test: 15 mL/min**

Visible in the video still is the initial cook off of propellant that occurred just after injection had stopped. During this time, the propellant gathered on top of the catalyst bed was vigorously boiling caused by gaseous reaction products traversing through the pooled propellant in the upstream direction back toward the injector. This allowed new unreacted propellant to come into contact with reaction sites in the catalyst. The process continued until enough of the propellant had boiled off where a sustained flame could be held on top of the catalyst bed at approximately 35 seconds into the run.

The advantages of injecting finely atomized HAN-based monopropellant was demonstrated in the test shown in Figure 4.6. In this experiment, two catalysts were used with a target preheat temperature of 420°C and a propellant flow rate of 5 mL/min. During testing, the injector atomized the HAN-based propellant for the first 3 seconds of the run and normal reactions occurred as shown in the temperature vs. time graph in Figure 4.6. After 3 seconds, atomization stopped and propellant droplets fell on the catalyst face which quenched the reaction and flooded the catalyst. This is seen in the sudden flat lining in the temperature of the downstream catalyst face 15 seconds into the test as shown in the figure. The unreacted propellant then proceeded to ignite uncontrollably as seen in the dramatic spike in the temperature profile of the test and the corresponding frame taken from video of the test. By finely atomizing the monopropellant, this test showed that a controlled reaction and burn can be initiated at preheat temperatures lower than that needed if the propellant was not atomized.

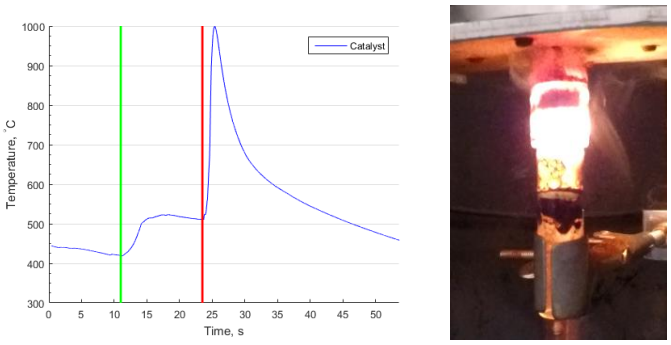

Figure 4.6. **Quartz flow-through test: 5 mL/min**

Chapter 5. DEVELOPMENT OF THE WORKHORSE MICROTHRUSTER

5.1 PURPOSE

The following describes the development of a laboratory scale 0.1 – 1 Newton HAN-based monopropellant workhorse microthruster. Utilizing the thermochemical data provided by the sponsors, the rocket thruster operating conditions and performance characteristics were determined for the final design. Transit times in both the catalyst bed and rocket chamber for flow rates of interest to microthrusters were also estimated. Factors of safety for the combustion chamber were evaluated based on worst case scenarios which led to preliminary thruster designs that could be readily fabricated and tested in the laboratory. Results of these theoretical considerations are discussed, followed by the modeled thruster concept, and finite element analysis thermal modeling.

5.2 WORKHORSE MICROTHRUSTER DESIGN REQUIREMENTS

The primary design requirement of the workhorse microthruster was to operate at flow rates between 2 and 20 ml/min with an initial target operating chamber pressure of approximately 21 bar (305 psig). The design required the ability to utilize various nozzle throat diameters to accommodate changes in flow rate and desired chamber pressure. The combustion chamber was required to be sized such that it could accommodate from one to three cylindrical monolithic foamed-metal catalysts, each of which are 12.7 millimeters in diameter and 7.2 millimeters in height. The exact number of catalysts to be used in testing was dependent on the results from flow-through testing. The catalyst bed required the ability to be heated in excess of 400°C using an external heat source. Provisions to minimize the potential for catalyst poisoning at the expected operational temperatures due to leeching of the chamber walls was to be incorporated. Pressure

and temperature instrumentation ports was to be included to enable monitoring of the flow upstream and downstream of the catalyst bed as well as the catalyst bed temperature.

5.3 WORKHORSE MICROTHRUSTER CONCEPT

The microthruster was designed for various injector flow rates, chamber pressures, porting for the required instrumentation, and catalyst bed heating via an externally applied electric band-heater. The schematic in Figure 5.1 shows a single cylindrical catalyst held within an inner sleeve having a slight step to retain and facilitate its exact positioning and quick removal. The sleeve and corresponding custom made spacer within the catalyst retention cavity were constructed of alumina (aluminum oxide) to minimize the potential for catalyst poisoning during preheat and operation. Materials were selected to minimize chemical reaction when in contact with both unreacted HAN-based propellant and its corresponding combustion products [5]. The sleeve slipped within the main combustion chamber body, which served as the pressure vessel and had accommodations for several instrumentation ports which included three pressure transducers, two in the combustion chamber downstream of the catalyst bed and one upstream of the catalyst bed near the injector.

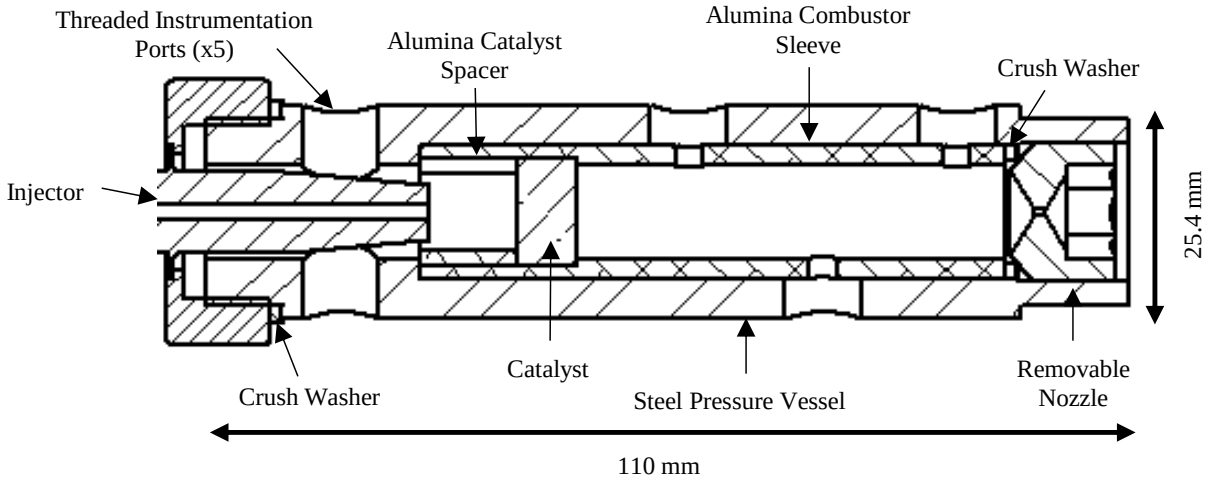

Figure 5.1. **Workhorse microthruster schematic**

Temperature instrumentation ports included one near the injector, two at the catalyst bed, and one in the combustor downstream of the catalyst bed. The removable nozzle was threaded into the recess at the end of the combustion chamber to press against a crush washer to retain the alumina sleeve and seal the combustion chamber. The threaded nozzle will prolong the operational lifetime of the microthruster over the course of testing by providing an easy means of replacing a burned out or otherwise damaged nozzle and allow a methodology for testing fixed flow-rate thruster operation at various chamber pressures. The injector was held with a retaining nut on external threads upstream of the catalyst bed and the injector face was positioned approximately 10 millimeters from the front of the catalyst. Complete drawings can be found in Appendix B.

5.4 WORKHORSE MICROTHRUSTER SIZING

5.4.1 *Nozzle Throat Sizing*

A combustion chamber diameter of 11 millimeters was chosen based on the catalyst bed form factor and allow the catalyst bed to rest on a machined step in the combustor. The chemical composition and enthalpy of formation of the propellant were used in the NASA Chemical Equilibrium with Applications (CEA) computer program to determine combustor properties over a range of operating pressures and flow rates. The adiabatic flame temperature was determined to have very little variation across flow rates and chamber pressures. The value found will be used to determine if complete decomposition and reaction of the HAN-based propellant has occurred. Using the combusted propellant properties from CEA, the relationship between nozzle diameter and mass flow rate was determined for the desired chamber operating pressure of the test. Using these data provides a means to readily determine nozzle throat diameter for a wide range of operating conditions.

5.4.2 *Combustor Length*

Combustion chamber length was determined with empirical characteristic chamber length, L^* guidelines for thrust chambers and the relation in Eq. 5.1, where V_c is combustion chamber volume and A_t is the nozzle throat area.

$$L^* = \frac{V_c}{A_t} \tag{5.1}$$

The characteristic chamber length L^* can vary between 0.8 and 3.0 meters for bipropellant rocket engines while monopropellant thrusters have characteristic lengths typically slightly higher [5]. This is because monopropellants have an extra reaction step with the catalyst bed to decompose the molecule. Without experimental data for monopropellant microthrusters using HAN-based monopropellant and to promote complete combustion at all flow rates and chamber pressures of interest, an L^* near the upper range was selected to be used as an initial test platform with plans to investigate shorter characteristic chamber lengths after initial testing. Using the prescribed chamber inner diameter of 11 millimeters and the range of nozzle throat diameters as determined from CEA, the combustion chamber length for varying nozzle throat diameters was then determined.

After extensive hot-fire testing, a combustor insert was developed to reduce the combustor volume. The combustor volume reducing insert was used to determine the effect the characteristic chamber length on HAN-based monopropellant combustion properties and to increase the pressure responsivness of the thruster. The installed insert can be seen in the schematic of Figure 5.2. The insert, constructed of SS316L, reduced the effective combustor volume with a single catalyst by roughly 65%. Utilizing the existing nozzle threads at the back end of the thruster, the combustor insert threaded in and was sealed in the same manner as the nozzle with a crush washer. A new nozzle was then installed into the insert and was sealed with commercial thread sealant. One drawback of using the combustor insert during testing was it reduced the downstream catalyst intrumentation ports to a single port. As a result, in tests using the insert, only a single temperature measurement was obtained from within the combustor chamber downstream of the catalyst bed.

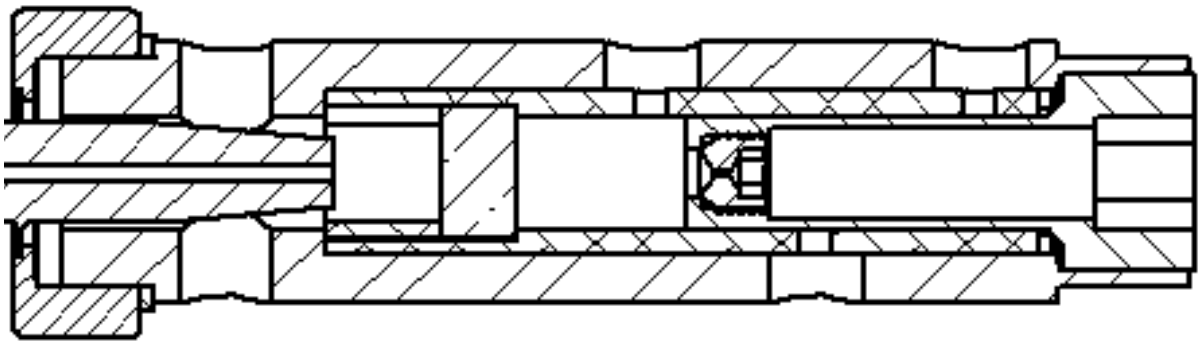

Figure 5.2. **Workhorse microthruster schematic with insert**

5.4.3 *Monopropellant Residence Time*

Propellant residence time t_s, was another parameter considered in the design of the workhorse thruster. This is average time spent by each molecule in the combustion chamber. In order to reach complete combustion which includes vaporization, activation, and burning, the minimum residence time must be met. Typical residence times have values of 0.001 to 0.040 seconds with the choice of propellant and design of the combustion chamber playing a considerable role in its

determination [5]. The residence time is given by Eq. 5.2 where t_s is the average propellant residence time, $\dot{m}$ is the mass flow rate, and υ is the specific density of the products from combustion.

$$t_s = \frac{V_c}{\dot{m}\upsilon} \tag{5.2}$$

The values calculated for the initial combustor length tend on the higher side of the typical values. Having a higher propellant residence time may lead to increased opportunity for the combustion products to react with the chamber walls; however, without previous experimental data to determine the minimum residence time of HAN-based monopropellant, the workhorse microthruster was designed to provide a higher residence time than likely needed to promote complete propellant combustion at all flow rates.

5.4.4 *Pressure Vessel Sizing*

The wall thickness of the combustion chamber was sized such that it can be capable of withstanding the maximum pressure rise expected during a constant volume combustion process within a closed combustion chamber with a margin of safety. This condition arises when the propellant does not ignite immediately upon injection and proceeds to react in a single event. A CEA constant volume combustion analysis with expected propellant injection volumes was conducted to determine a maximum combustion chamber pressure of 970 bar (14,100 psig) is produced in such an event. To determine the burst pressure of the thruster design, the stress was determined using closed end thick walled cylinder equations given by Eqs. 5.3 - 5.5 where σ_a is

the axial stress, σ_h is the hoop stress, σ_r is the radial stress, P_i is the internal pressure, P_o the external pressure, r_i the internal radius and r_o is the external radius.

$$\sigma_a = \frac{P_i r_i^2 - P_o r_o^2}{r_o^2 - r_i^2} \tag{5.3}$$

$$\sigma_h = \frac{P_i r_i^2 - P_o r_o^2}{r_o^2 - r_i^2} - \frac{r_i^2 r_o^2 (P_o - P_i)}{r^2 (r_o^2 - r_i^2)} \tag{5.4}$$

$$\sigma_r = \frac{P_i r_i^2 - P_o r_o^2}{r_o^2 - r_i^2} - \frac{r_i^2 r_o^2 (P_i - P_o)}{r^2 (r_o^2 - r_i^2)} \tag{5.5}$$

Stresses were calculated at the internal radius and using an external pressure of zero. Due to additional design considerations that will be discussed in the next section, a value of 15.9 millimeters was used for the inside diameter of the thrust chamber. Including a temperature correction factor of 0.8 and using properties of SS316L, it was determined an outside diameter of 25.4 millimeters would give a factor of safety of 1.6 for the case of a constant volume combustion within a closed combustion chamber. During normal operating pressure of up to 21 bar (305 psig), the workhorse microthruster pressure vessel had a factor of safety of 70.

5.5 Thermal Modeling

5.5.1 *Setup*

The thermal analysis of the microthruster design was conducted using ANSYS Mechanical V16.2. Material properties were selected to match those used in the design of the workhorse microthruster thruster; this included SS316 for the microthruster body and electric band heater, 6Al-4V-Ti for the injector and injector nut, and rhenium with a density of 50% to simulate the porosity characteristics of the foamed metal catalyst. The thermal characteristics of the

microthruster design were investigated under two different thermal conditions; the first was a steady state operation condition where the catalyst was held at a temperature of 400°C to determine the temperature gradient and field of the workhorse thruster when preheated; the second was a transient preheat to a catalyst preheat temperature of 400°C starting from an ambient temperature of 22°C.

The steady state and transient thermal analysis were carried out using a quarter symmetry model with an element size of 1 millimeter. In order to reduce computation time, the thermal model design as seen in Figure 5.3 was simplified by incorporating the combustor sleeve and nozzle into the main body, removing the instrumentation ports, and modeling the electric band-heater as a cylinder with an outer diameter of 34 millimeters.

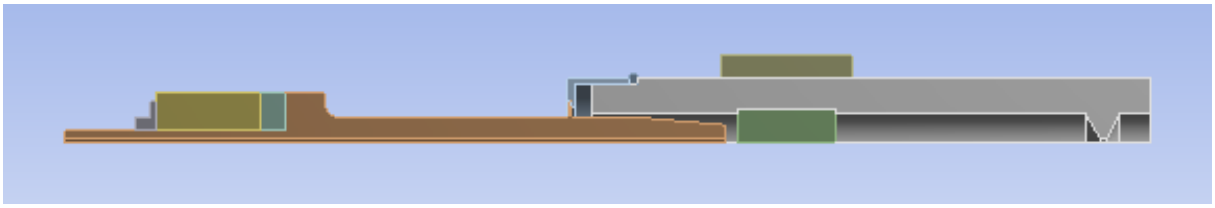

Figure 5.3. **FEA microthruster model**

The initial thermal conditions for the microthruster were set to standard temperature and pressure conditions of 22°C and 1 atmosphere. Constant convection coefficients of 10 W/m^2-K were used on exposed surfaces and a radiation emissivity value of 0.19 was used for the stainless steel and titanium surfaces. Internally, surface to surface radiation conditions were defined for the pre-catalyst chamber and combustion chamber, with an emissivity of 0.5 for the catalyst faces. Bench tests with the band-heater found that it had a power draw of 151 watts, with a volume of approximately 10.2 $centimeters^3$, resulting in a power density of 1.49×10^7 W/m^3, thus this value was used in the thermal model as internal heat generation provided by the band heater.

5.5.2 *Transient Preheat Thermal Analysis*

The results of the transient thermal analysis can be seen in Figure 5.4 showing the thermal profile of the FEA workhorse microthruster when the catalyst bed has reached 400°C. The thermal analysis shows the band heater has the ability to preheat the catalyst to 400°C while retaining a reasonable temperature at critical locations in the injector. Nonetheless, the presence of a large thermal gradient along the length of the injector may impact the performance of the injector; the effects of which are to be determined during hot-fire testing of the workhorse system.

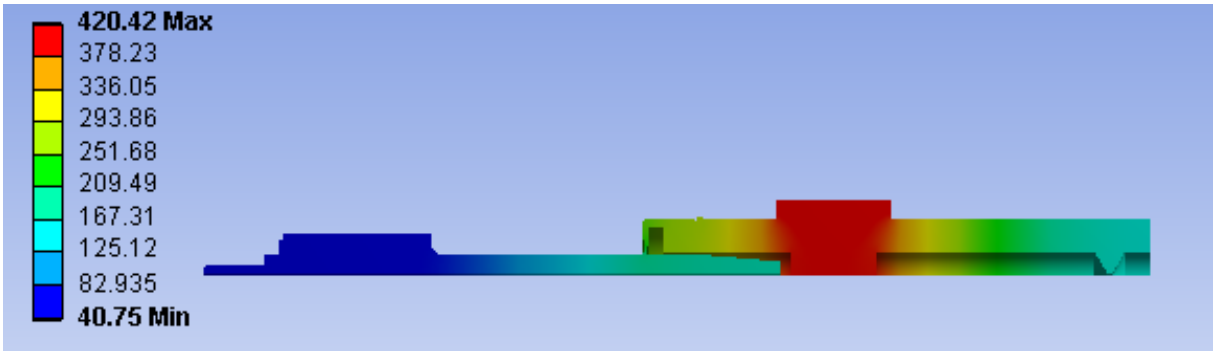

Figure 5.4. **Transient thermal profile of the workhorse microthruster**

Shown in Figure 5.5 is the time-temperature data for the transient preheat analysis for four locations on the FEA model of the workhorse system. The locations selected were the catalyst-bed temperature, and three locations spaced across the length of the injector to capture the temperature profile of the injector. The time the system took to preheat the catalyst bed to a temperature of 400°C was 630 seconds (10.5 minutes). The time-temperature response of the points along the length of the injector showed there is considerable thermal impedance in the injector system and that there is an approximate 4 minute delay between when the heater is given power and a temperature response is seen in the rear part of the injector.

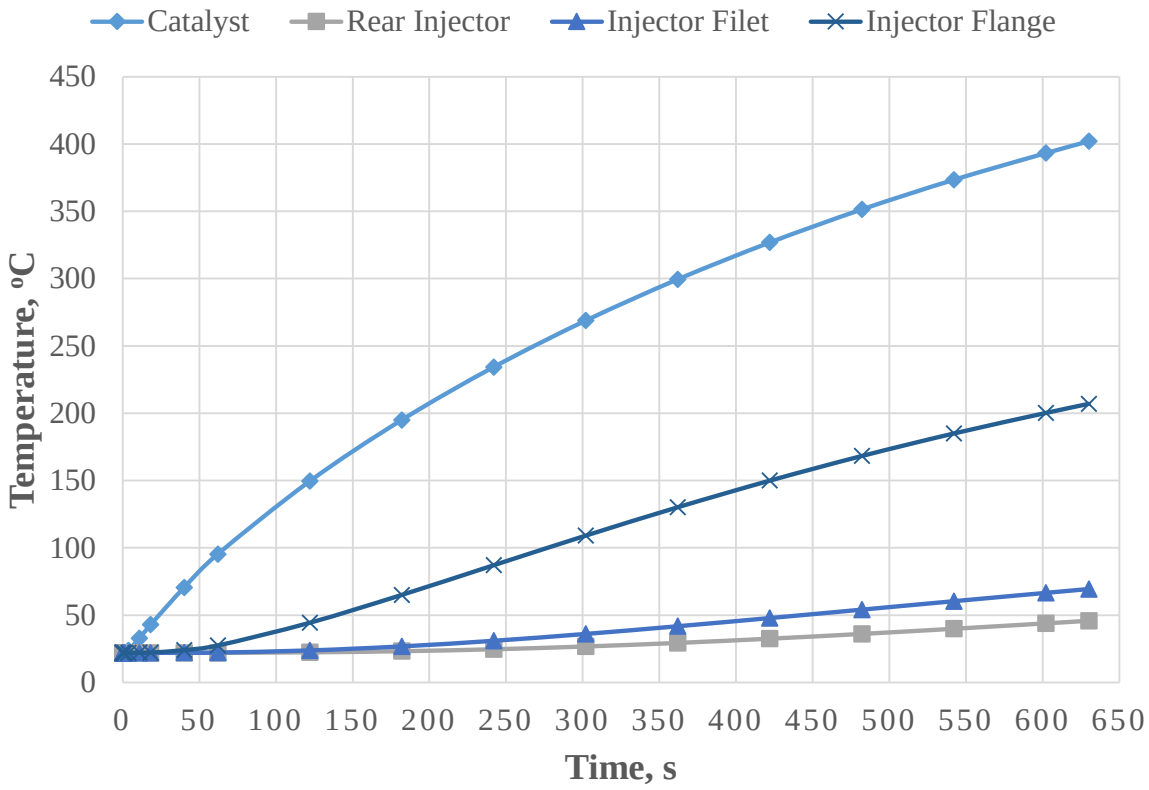

Figure 5.5. **Temperature during preheat for locations along the injector**

5.5.3 *Steady State Thermal Analysis*

Under steady-state conditions the predicted temperature field of the workhorse microthruster is shown in Figure 5.6. The required band heater power to maintain a catalyst temperature of 400°C was 9.0 x 10^6 W/m^3. By using the volume of the CAD created band heater, this determined the power input to be 91.7 Watts. This was 60% the maximum available power of the band heater. As in the transient thermal analysis, minimal thermal soak back into the injector was observed. However, comparing the temperature at the flange where the injector attaches to the thruster which shows an approximate value of 250°C and that of the rear of the injector, a large temperature gradient of approximately 150°C is apparent.

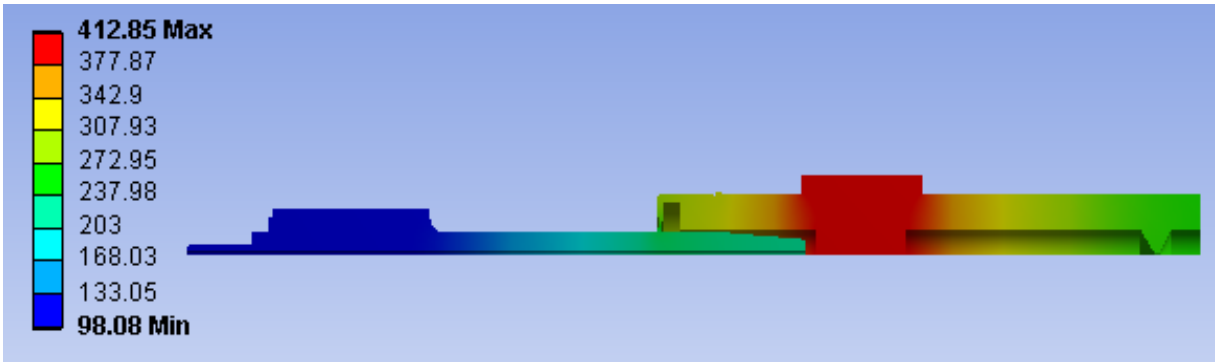

Figure 5.6. **Steady state thermal profile of the workhorse microthruster**

5.5.4 *Heat Flux into Injector Assembly*

The power dissipated through the injector was determined by monitoring the heat flux through a cross-sectional area of 71.3 millimeters^2 in close proximity to the flange of the injector. The heat flux passing through the injector to the upstream flow control components during the preheat stage is seen in Figure 5.7. Under the steady-state operating condition where the catalyst was maintained at a temperature of 400°C, the heat flux through the injector was found to be 140 kW/m^2. This determines that 9.98 Watts must be dissipated through the injector body in the form of radiative and convective heat transfer. While the system may never reach this condition, it was a useful quantity to know to be able to determine the cooling power needed to dissipate the thermal soak into critical injector components in a steady state operational condition. During the preheat stage, the maximum heat flux passing through the injector was found to be greater than that found in the steady state analysis due to the heater supplying 100 percent of its available power.

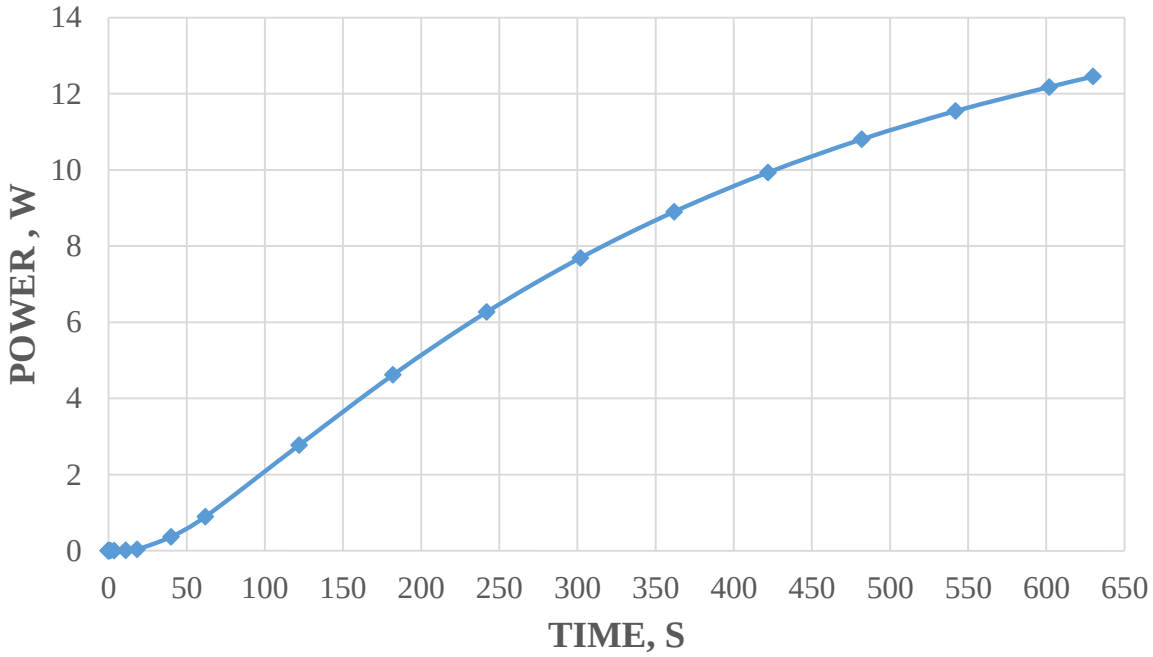

Figure 5.7. **Power dissipated through the injector system during preheat**

5.5.5 *Comparison with Testing*

Preheat and steady state temperature profiles of the actual workhorse microthruster system are seen in Figure 5.8. Comparing to the ANSYS FEA transient thermal results in Figure 5.5, the time required to preheat was approximately 60% greater taking the actual system close to 1000 seconds (16.7 minutes) for the catalyst bed to reach 400°C. This preheat test was conducted with the PID controller turned off so that the heater was supplied with its maximum amount of available power. The experimental test temperatures were also higher than that predicted in the FEA model. At the flange on the injector, where the injector is attached to the workhorse thruster, the recorded temperature was 80°C higher than expected. The rear of the injector was also approximately a factor of two greater in temperature than that obtained through the analysis.

Although the transient thermal predictions are off, the steady state temperatures shown in the table in Figure 5.8 show a good correlation at the injector flange and rear injector when compared

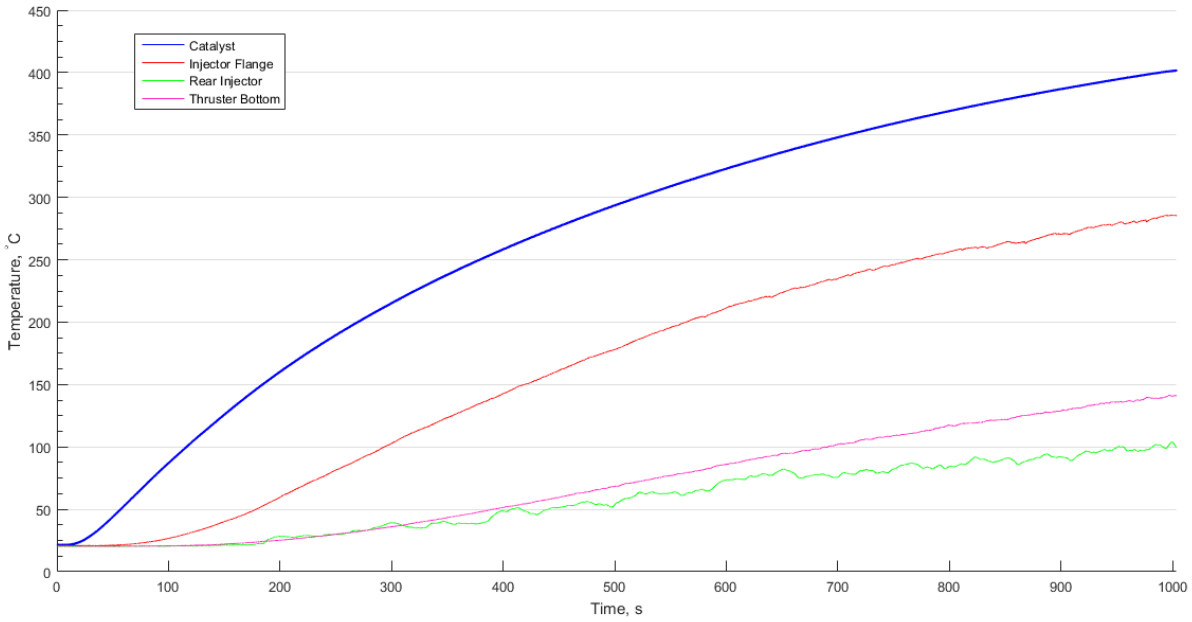

Time	Catalyst	Injector Flange	Rear Injector	Thruster Bottom
Steady State	400°C	293°C	108°C	174°C

Figure 5.8. **Temperature of microthruster during preheat and steady state**

with the thermal image profile in Figure 5.6. However, the downstream side of the workhorse thruster shows approximately 100°C less than what was expected from the FEA thermal analysis.

The discrepancies between the predicted temperatures and the actual test temperatures may have arisen from a number of causes. The leading belief was thermal contact resistance barriers between parts in the workhorse system was not modeled in the FEA analysis. This would have the effect of increasing the time required to preheat the catalyst and produce lower predicted temperatures in the transient analysis. Another parameter that may have added error to the analysis was the use of constant nominal emissivity and convection coefficients used in the analysis. This would play a role in the magnitude of the thermal gradient seen in the system which would show up when comparing the results at the extreme ends of the model, such as at the downstream end of the workhorse microthruster.

Chapter 6. WORKHORSE MICROTHRUSTER TESTING

6.1 PURPOSE

Initial tests examined the required input power for catalytic ignition at a specified catalyst bed temperature as a function of propellant flow rate. Temperature and pressure measurements will indicate the degree of combustion completion within the chamber length provided.

6.2 TESTING HARDWARE AND SOFTWARE

6.2.1 *Hardware*

An aluminum test stand was constructed to be used as a test platform in all atmospheric tests with the workhorse thruster. Seen in Figure 6.1, the stand was constructed with two rings, one of which acted as a base and allowed the three threaded vertical rods to be installed. The workhorse microthruster was then installed with a thin circular plate in-between the injector mounting nut and the upstream instrumentation ports onto the vertical rods. This plate added additional securement of the thruster during instrumentation and assembly of the combustor/nozzle prior to a test. A second ring was then placed on the vertical rods, this ring had three thumb screws which clamped down onto the injector nut which provided a secure hold onto the workhorse microthruster. Tests were conducted in a downward firing orientation with the test stand placed on top of a steel topped table.

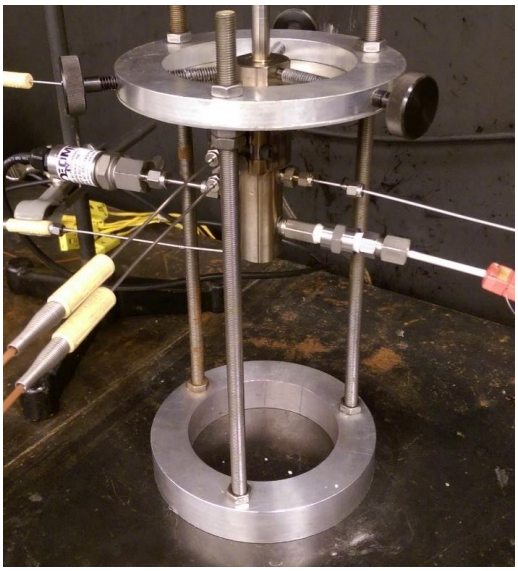

Figure 6.1. **Workhorse microthruster test stand**

For hot-fire testing of HAN-based monopropellant at the University of Washington, tests were conducted within a secure lab environment under a fume hood. Even though HAN-based propellant are “green” propellants, partial decomposition of the propellant could result in hazardous gases generated. The fume hood was blocked off with plastic sheeting on three of the four sides to enhance containment of the exhaust gases.

The preheat operation for all hot-fire tests was performed using a commercial off the shelf band heater from Tempco. The heater utilized was a Mi-Plus® band heater which provided the high watt density needed for the form factor of the workhorse system. The particular heater purchased had a 1 inch inside diameter and was 1 inch in length; this heater provided a power of 150 Watts with a maximum temperature rating of 760°C. The heater operation was controlled through a proportional-integral-derivative (PID) controller, the catalyst temperature thermocouple was utilized for both data recording and had a y-split to be used as the temperature input source for the PID controller. This allowed preheat set point temperatures to be programmed in to create a steady state temperature of the workhorse thruster prior to testing.

The propellant feed system utilized a positive displacement syringe pump and stainless steel syringe obtained from New Era Pump Systems as shown in Figure 6.2. The pump was capable of a maximum flow rate of 38 mL/min and 200 lbf at low rates and 100 lbf at high rates. Coupled with a 5 milliliter syringe with an inside diameter of 12.7 millimeters, the maximum feed pressure capacity was between 35 to 70 bar (510 - 1020 psi) depending on the flow rate of interest.

Figure 6.2. **Propellant feed pump**

1/8 inch Peek tubing was used to connect the propellant feed syringe to the injector mounted on the workhorse microthruster.

A series of electromagnetic valves was constructed in order to aid in filling, bleeding, and purging the feed system. Pressure and temperature data were also incorporated into the feed system in order to record pre-injector propellant flow properties.

Figure 6.3 shows a diagram of the setup which included two three-way electromagnetic valves. The valve nearest to the syringe was used for filling and bleeding of the syringe while the valve nearest to the injector was used for bleeding of the feed line. Two electromagnetic isolation valves are also depicted in the schematic, the first is in line with the three-way valves and was used to isolate the injector side of the feed system from the propellant in the syringe. The second isolation valve is located at a tee just downstream of the first isolation valve, this valve controled the nitrogen purge line.

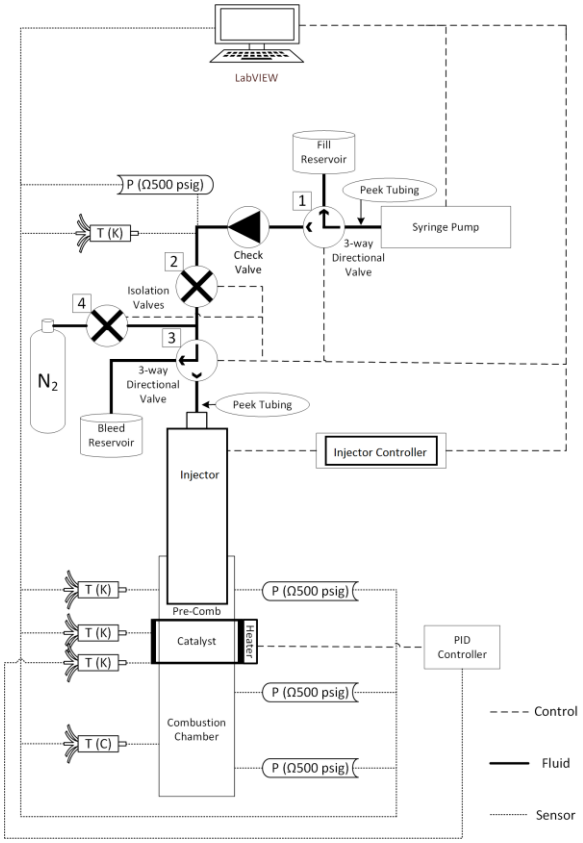

Figure 6.3. **Workhorse PID Diagram**

During hot-fire microthruster testing, it was found the feed valve system could not be fully bled with residual air pockets residing within the temperature and pressure ports, purge line, and valve mechanisms. Uniform feed and bleed was accomplished by simplifying the feed system down to its core components of a syringe that is directly attached to the injector by a length of Peek tubing.

During testing, this configuration proved to be the most effective at obtaining a fully bled system, an additional benefit of proceeding with this solution was the propellant dead volume in the feed system dramatically reduced from the reduction in fluid flow paths.

Data acquisition was carried out through a National Instruments CompactDAQ® system. The DAQ made use of separate modules capable of performing various tasks. Modules used for this experiment were two voltage measurement modules, one for the 0 to 5 volt pressure transducers and the other for Type-C thermocouple data which was preconditioned using an in-house built instrumentation amplifier; both modules were able to sample up to a nominal 10,000 samples/s. A standard thermocouple module was used for reading the Type-K thermocouples with a maximum sample rate of 95 samples/s. A relay module was also used for controlling the electromagnetic valves while they were in use.

6.2.2 *Software*

A LabVIEW® script and control interface were developed to read in the temperature and pressure data as well as controlling the feed system. The control panel allowed real time viewing of the pressure and temperature during a test via three different scrolling graphs: one for pressure and separate graphs for Type-C and Type-K thermocouple data. Raw and filtered data were available from the pressure and Type-C sensors. Feed pump parameters built into the control panel included flow rate and volume to be injected as well as more advanced options for use in pulsed mode testing and flow rate ramping. These options included pulse width and pause time, number of pulses, specific injector parameters to be run between and after injection, propellant flow rate ramp start and end rates, and the volume and total time of ramping. A full overview of the control panel can be seen in Appendix A with operating instructions and procedures. To process the data,

Matlab® was implemented to read in the temperature and pressure output files from LabVIEW®, the data extraction script can be seen in Appendix C.

6.3 CONFIGURATION

Preliminary tests were configured with two pressure transducers (0 - 34.5 bar range) installed in the combustor section downstream of the catalyst bed. After these tests, it was deemed that one transducer was sufficient to characterize the combustor pressure and two thermocouples could then be installed in the combustor section, one just after the cat-bed and another just before the throat. Other instrumentation that remained the same for this test series was a Type-K thermocouple in contact with the outside cylindrical edge of the upstream catalyst to monitor its temperature during preheat and testing. Two more Type-K thermocouples were placed upstream of the catalyst, one in contact with the outside face of the alumina catalyst spacer and the other exposed to the upstream volume on the side of the injector head. The pressure upstream of the catalyst was monitored to determine the magnitude of the pressure differential across the catalyst. Throughout a wide range of operating parameters, it was determined that there was no significant pressure drop across the catalyst bed, as such pressure data are presented from only the combustor transducer downstream of the catalyst bed in tests that incorporated multiple pressure transducers.

6.4 OPEN NOZZLE HOT-FIRE TESTS

The first propellant tests conducted in the workhorse thruster were an extension of the flow-through testing. The male threaded piece from the stainless steel flow-through holder was inserted into the rear of the thruster in place of a nozzle. This series of tests had several different purposes; one of which was to run a shakedown test of the control panel for the data acquisition system and feed system to ensure reliable operation and workability, the other was to examine the

monopropellant reaction with the catalyst at various preheat temperatures to draw insight on what the initial operating envelope may be for the system.

Figure 6.4 presents the temperature data from a test conducted at a catalyst bed preheat temperature of 415°C with a propellant flow rate of 1 mL/min, a representative frame from the video taken of the test is shown. During this test, the exhausted products were not visually discernible. Shown in red in the plot, the catalyst temperature experienced a slow but steady temperature rise from its preheated temperature of 415°C up to its maximum temperature of 530°C. The large difference in catalyst temperature history between these tests and those conducted in the quartz flow-through combustor may be due to the effects of a large amount of heat being transferred to the inside walls of the workhorse thruster; this could also be compounded by the low flow rate used during this test sequence.

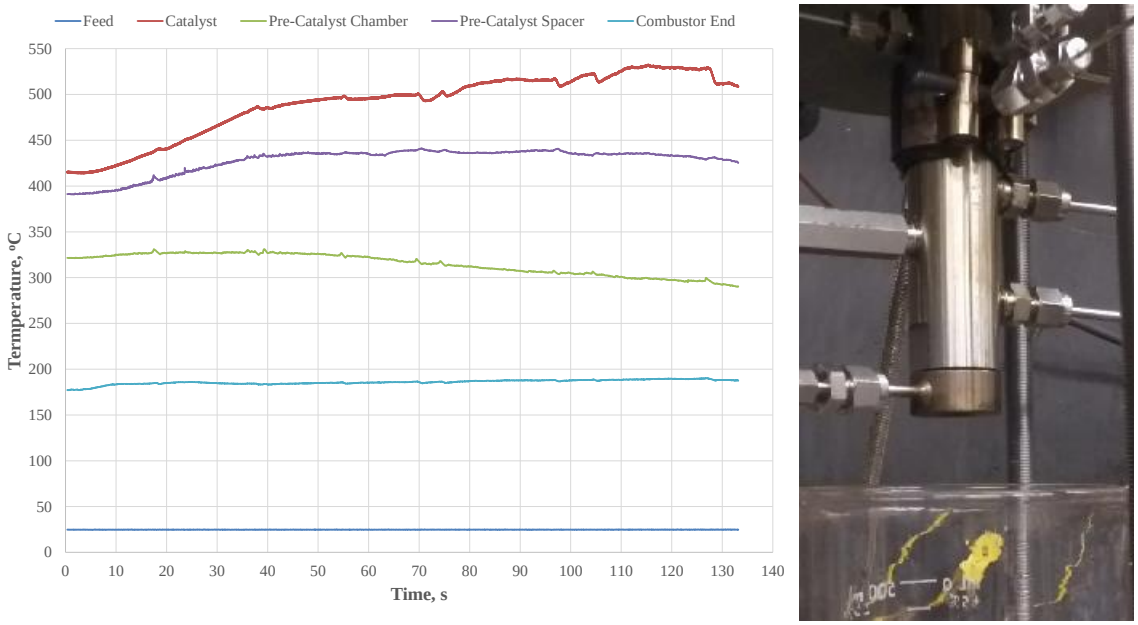

Figure 6.4. **Open combustor testing, preheat 415°C**

A test performed at catalyst preheat temperature of 325°C with a propellant flow rate of 1 mL/min is shown in Figure 6.5. This test showed a steady catalyst temperature rise up to 390°C. During this time the thruster exhausted grayish smoke from the nozzle-less combustor exit; this is seen in the representative still taken from the test as shown in the picture on the right in Figure 6.5. Once the catalyst bed thermocouple reached 390°C, the grayish plume became clear and was similar to that seen in the test at a catalyst bed preheat temperature of 415°C. This indicated a change in the decomposition and reaction of the HAN-based propellant occurred. Upon the catalyst reaching 390°C, the temperature then abruptly increased to 510°C and after approximately 20 seconds the catalyst bed temperature reached thermal equilibrium and leveled off for the remainder of the test.

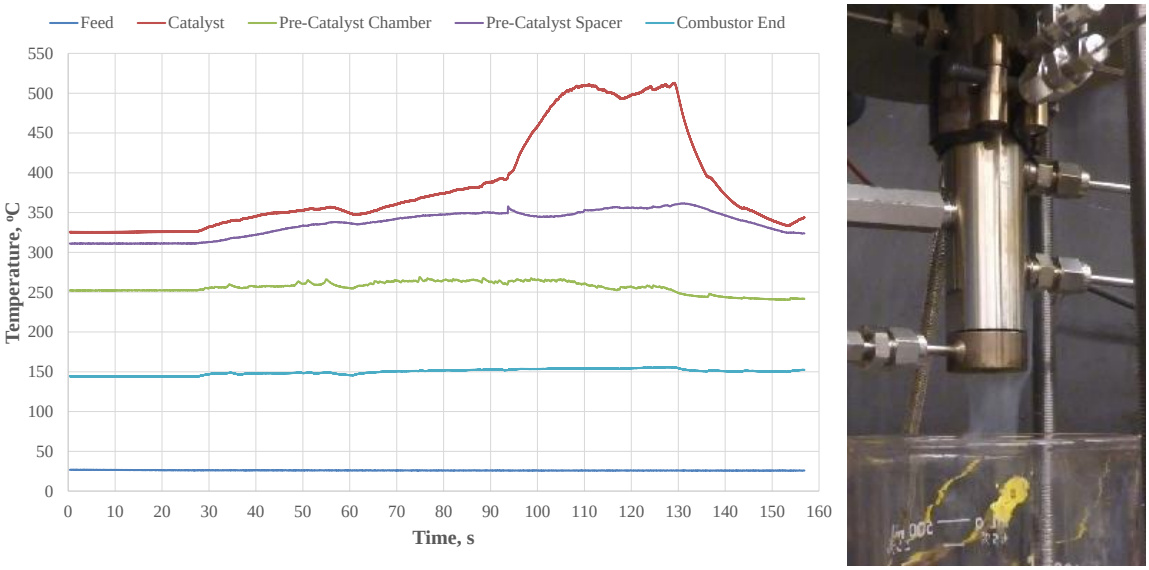

Figure 6.5. **Open combustor testing, preheat 325°C**

The dramatic change in the temperature profile of the catalyst temperature during this test signifies that initially the monopropellant was only partially decomposing and reacting when the atomized spray from the injector came into contact with the catalyst bed. Once the catalyst bed reached a critical temperature for the propellant, a higher degree of reactions started to take place resulting in the increase in temperature. In neither of these tests did the combustor temperature or

catalyst temperature approach the calculated adiabatic flame temperature. Discussed previously, this could be caused by a combination of low propellant flow rate and the thermal mass of the workhorse microthruster system. Pressure effects may also play a role in the decomposition of the HAN-based monopropellant used and is investigated further in the pressurized hot-fire testing in the workhorse microthruster.

6.5 Pressurized Hot-Fire Test Results

Testing has been conducted with the workhorse microthruster system as detailed in the following sections. This experimental series mainly focused on determining the temperature and pressure characteristics of steady state operation. The results from preliminary pulsed operation testing are presented here as well.

6.5.1 *Single Catalyst Test without Volume Reducing Insert*

Data from a run conducted in the standard configuration without the combustor volume reducing insert are presented in Figure 6.6. For this test, the cat-bed preheat was 400°C and propellant flow rate was 20 mL/min. The pressure data shown in black indicate the workhorse thruster had an initial pressure rise rate of approximately 180 psi/s. After the initial large increase in chamber pressure a slow steady rise at 5 psi/s is seen which increases up to a maximum pressure of approximately 340 psig. The slow rise in the pressure data is believed to be caused by thermal heat transfer effects with the combustor chamber walls of the workhorse thruster.

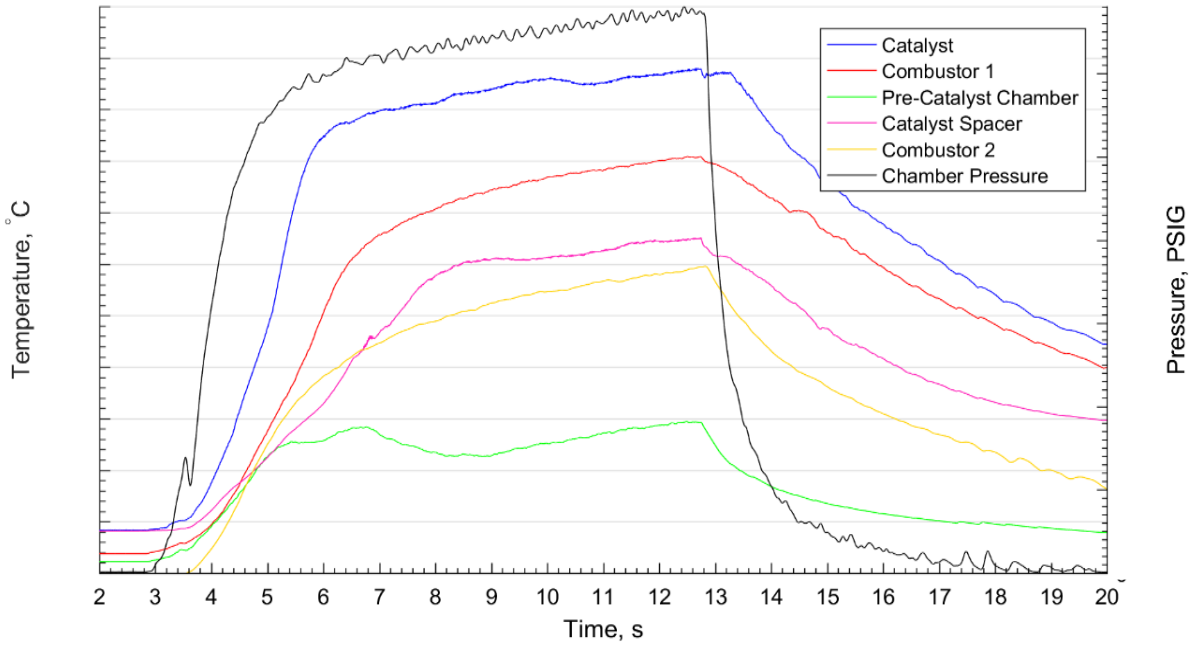

Figure 6.6. **Microthruster test: 20 mL/min flow rate without chamber insert**

The maximum catalyst temperature during the 10 seconds of injection for the run was approximately 1300°C, and is one of the highest recorded temperatures seen during testing. The instrumentation in the downstream chamber consisted of one Type-K thermocouple in the instrumentation port just downstream of the catalyst bed, labeled Combustor 1; and a Type-C thermocouple installed in the instrumentation ports just upstream of the removable nozzle labeled Combustor 2. The difference in recorded temperature between Combustor 1 and 2 without the insert installed shows there is a thermal gradient inside the combustor volume downstream of the catalyst bed. The thermal gradient was most likely caused by thermal interactions with the chamber walls which transferred heat from the combustion products. This was also seen by the temperature increase throughout the test, which indicated that heat transfer to the walls may be a factor. The temperatures in the catalyst and post-catalyst regions were less than that predicted for the adiabatic flame temperature of the HAN-based monopropellant expected from the test. Whether this was due to heat transfer losses or incomplete combustion remains to be determined.

6.5.2 *Single Catalyst Test with Volume Reducing Insert*

Data from a typical run with a single catalyst with the volume reducing insert are shown in Figure 6.7. For this test, the catalyst bed preheat temperature was 400°C and propellant flow rate was 20 mL/min. The pressure data indicated an initial rise rate of 400 psi/s which more than doubled that found in tests without the chamber insert installed. The pressure data also had a smaller pressure drift during the steady state period of the run at approximately 3 psi/s, just under half that seen without the insert installed. At the conclusion of the run a pressure spike is seen in the data after the pressure in the combustor has dropped to 20 psig. This spike was caused by the propellant feed system relaxing after the syringe pump was shut off and a droplet fell from the injector face onto the catalyst bed. This has been mitigated by running a different injector profile at the end of the run such that a droplet does not form.

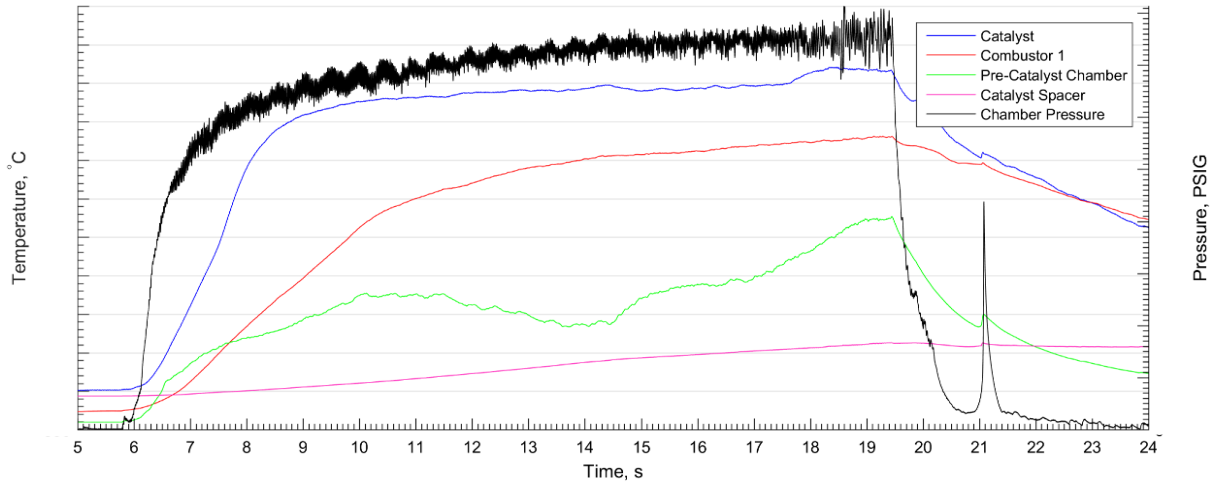

Figure 6.7. **Microthruster test: 20 mL/min flow rate with chamber insert**

The catalyst temperature shown in blue and downstream chamber temperature in red reached approximately 1200°C and 1150°C, respectively, with the catalyst reaching steady state after 2 seconds of propellant injection. Comparing the catalyst temperature data to the previous test show the catalyst temperature was lower in the test with the insert installed by approximately 100°C. The Combustor 1 data also showed a drop by approximately 50°C with the volume

reducing insert installed. A possible explanation for the lower catalyst and combustor temperature with the volume reducing insert is the residence time of the propellant is less in this configuration than without the insert installed. Given the overall lower temperatures than the calculated adiabatic flame temperature, incomplete combustion is believed to exist. With the insert installed, there was an approximate 65% reduction of the internal volume in region downstream of the catalyst bed. A smaller combustor volume would give the propellant less time to react after initial decomposition, thus providing a possible explanation for the lower temperatures seen from the reaction products.

The upstream pre-catalyst chamber temperature taken around the side of the injector presented in green shows some temperature instability within that region. However, comparing the temperature recorded there and that at the catalyst and in the combustion chamber, the measured temperature is much less in this region. This leads to the conclusion that the monopropellant was reacting within the catalyst bed with very little to no reactions occurring downstream of the catalyst or around the side of the injector head. There was also no evidence of pooling occurring on the catalyst as was seen in the see-through quartz reactor testing at these flow rates with or without the volume reducing insert installed. Evidence of this would have been elevated pressure and temperatures continuing after injection had stopped, as well as greater fluctuation in pressure and temperature data caused by irregular reactions.

6.5.3 *Frequency Analysis of Pressure Data*

In the pressure trace of Figure 6.7 an oscillatory signal was seen during the course of the run when the test had reached steady state operation. Using the Matlab® script found in Appendix D, the underlying frequency can be found in the pressure data and plotted as a time-frequency response as seen in Figure 6.8. The top plot shows a mean subtracted and normalized 5 second sample of the pressure signal from the run. The second plot depicts the component frequencies

found in the pressure trace; visible is a peak at approximately 0.5 Hertz which corresponds to the large slow oscillation seen in the pressure data. There is also a prominent rise in the 21 - 25 Hertz frequency range which links to the higher frequency wave pattern visible in the 5 second sample of data selected. The third graph displays the frequency spectrum of the signal over the time of the sample data and shows the time evolution of the frequency. At the start of the sample, the higher frequency was approximately at 25 Hertz; as time went on the frequency decreased to just over 20 Hertz. This phenomena is the reason why the second plot in Figure 6.8 has a sweep of frequencies between 21 and 25 Hertz. The slow drop in frequency can be explained by the heating of the gases inside of the thruster causing a change in sound speed.

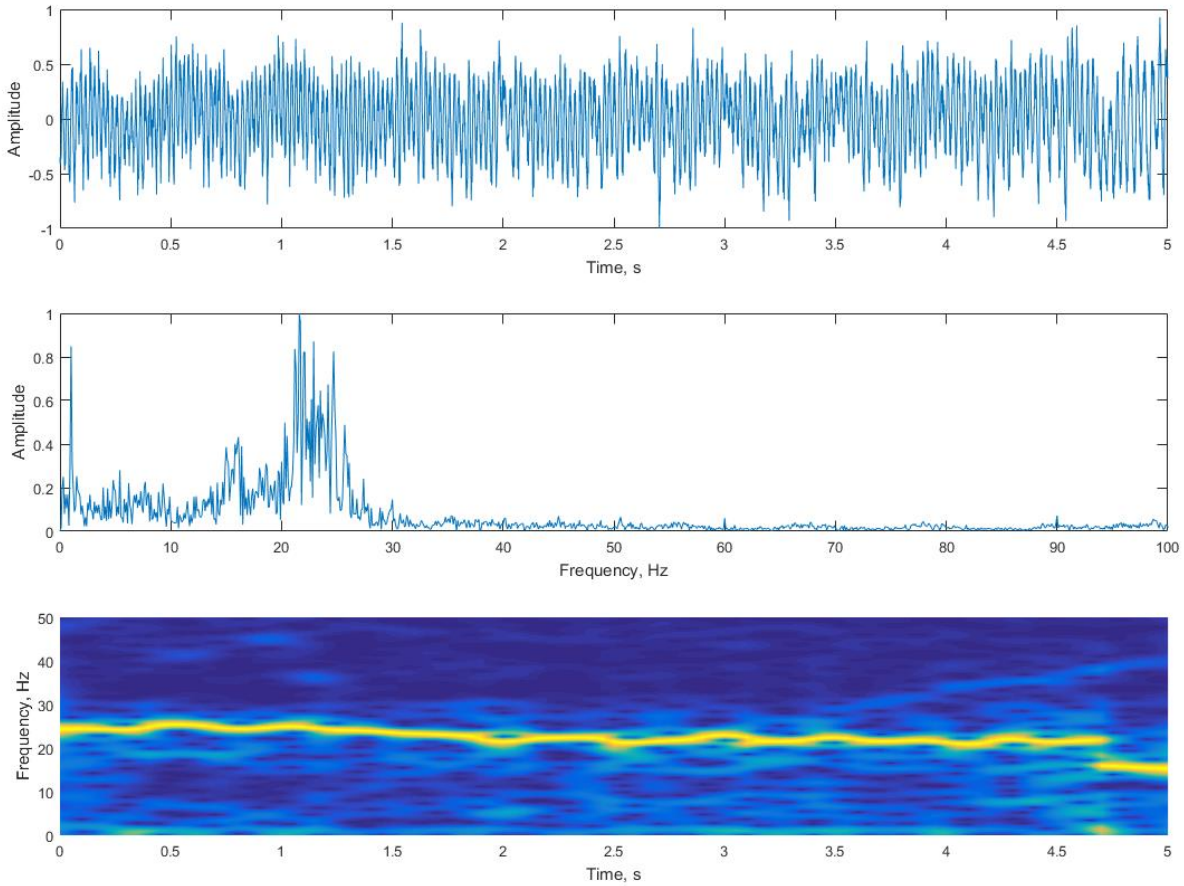

Figure 6.8. **Time-frequency response of workhorse pressure data**

6.5.4 *Single Catalyst Test Outlier*

Figure 6.9 represents a workhorse microthruster test that was an outlier in terms of the general trends that had been observed in the workhorse system. A single catalyst was installed and preheated to 400°C, the propellant flow rate was 2.5 mL/min with a target combustion chamber pressure of 3.8 bar (40 psig) using an appropriately sized nozzle throat diameter, the volume reducing insert was not installed.

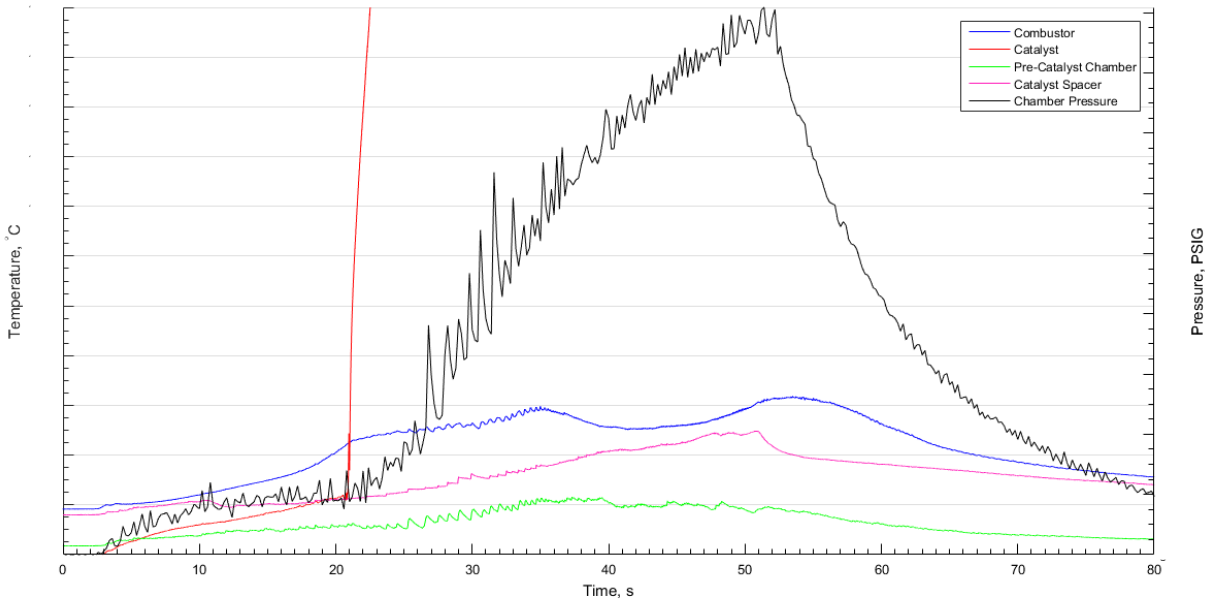

Figure 6.9. **Microthruster test: 2.5 mL/min flow rate**

The temperature and pressure time profiles are shown for the test. This test was conducted near the beginning of the workhorse microthruster test series and as such the instrumentation in the combustor section of the thruster consisted of one Type-K thermocouple and two pressure transducers, of which data from only one is shown. The combustor temperature profile had an immediate rise 22 seconds into the experiment. Subsequently the combustor temperature increased to beyond 1400°C and melted the exposed bead of the Type-K thermocouple. Comparing the temperature data elsewhere in the workhorse microthruster, it was apparent this combustion event only took place in the downstream portion of the catalyst combustor section, otherwise there would

have been evidence of a large temperature increase in the catalyst bed and upstream of the catalyst as well. Another aspect to note about the test depicted in Figure 6.9 is that the nozzle throat became partially blocked from products of combustion which resulted in the increase of the chamber pressure well above the expected 3.8 bar. This pressure increase coincided with the temperature spike in the combustor section.

6.5.5 *Single Catalyst Pulsed Testing*

Tests were also performed under pulsed operation with data from a representative pulsing test plotted in Figure 6.10. This test used the same configuration and flow parameters as presented in Figure 6.7 except in pulsed mode operation to examine the transients of the workhorse microthruster. The pulses were configured to have 1.5 seconds of injection followed by a 1.5 second pause. The chamber pressure rapidly rose in every pulse except for the first pulse. The weak and irregular first pulse was caused by the feed system bleeding out approximately 0.3 milliliters of air from the injector assembly.

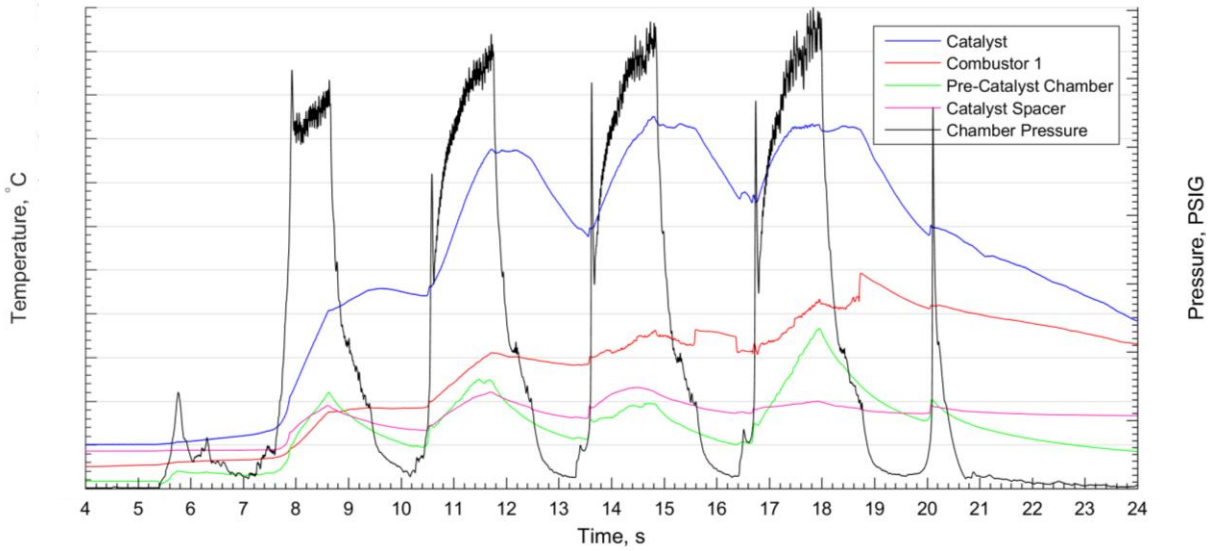

Figure 6.10. **Pulse test: 20 mL/min flow rate, 1.5 s pulse cycle**

Repeatable operation was seen to occur after three injection pulses where the chamber pressure and catalyst temperature became consistent from pulse to pulse. However, the combustor temperature continued to rise upon each consecutive pulse. This signaled all of the monopropellant was reacting within the catalyst bed and only products of reaction were continuing through the catalyst bed and into the chamber downstream of the catalyst. The combustor temperature was well below the theoretical combustion temperature and experimental temperatures seen during steady flow rate testing. During the pulsed operation, the catalyst reached a maximum temperature of approximately 1150°C, slightly lower than that found in steady state operation. Upon the last injection pulse, the chamber pressure rose to approximately 350 psig, slightly below that of the corresponding steady state operating pressure. Given a longer injection pulse, the trend in the pressure rise for the pulse test shows comparable pressures to those found in steady-state testing would have been obtained.

6.5.6 *Workhorse Thruster Combustion Efficiency*

A figure of merit for comparing the performance of the workhorse microthruster from test to test and to theory is by determining the experimental characteristic velocity, c^*. The experimental characteristic velocity can be calculated two ways; one of which is pressure based and is given by Eq. 6.1 where P_1 is the chamber pressure, A_t is the area of the nozzle throat, and $\dot{m}$ is the propellant mass flow rate. The other method is temperature based and is given by Eq. 6.2 where k is the ratio of specific heat, R is the individual gas constant, and T_1 is the temperature inside the combustion chamber of the thruster. The ratio of specific heat and individual gas constant were both determined theoretically through CEA. The experimental characteristic velocity can then be compared to the theoretical characteristic velocity as given in Eq. 6.3 where η is the combustion efficiency.

$$c^*_{exp} = \frac{P_1 A_t}{\dot{m}} \tag{6.1}$$

$$c^*_{exp} = \frac{\sqrt{kRT_1}}{k\sqrt{[2/(k+1)]^{(k+1)/(k-1)}}} \tag{6.2}$$

$$\eta = \frac{c^*_{exp}}{c^*_{theory}} \tag{6.3}$$

The combustion efficiency allows the direct comparison of the performance of the workhorse thruster across all of the tests conducted where a steady state temperature and pressure was reached. Figure 6.11 presents the combustion efficiency when compared to the operating chamber pressure during each respective test. The pressure based efficiencies are shown with blue diamonds

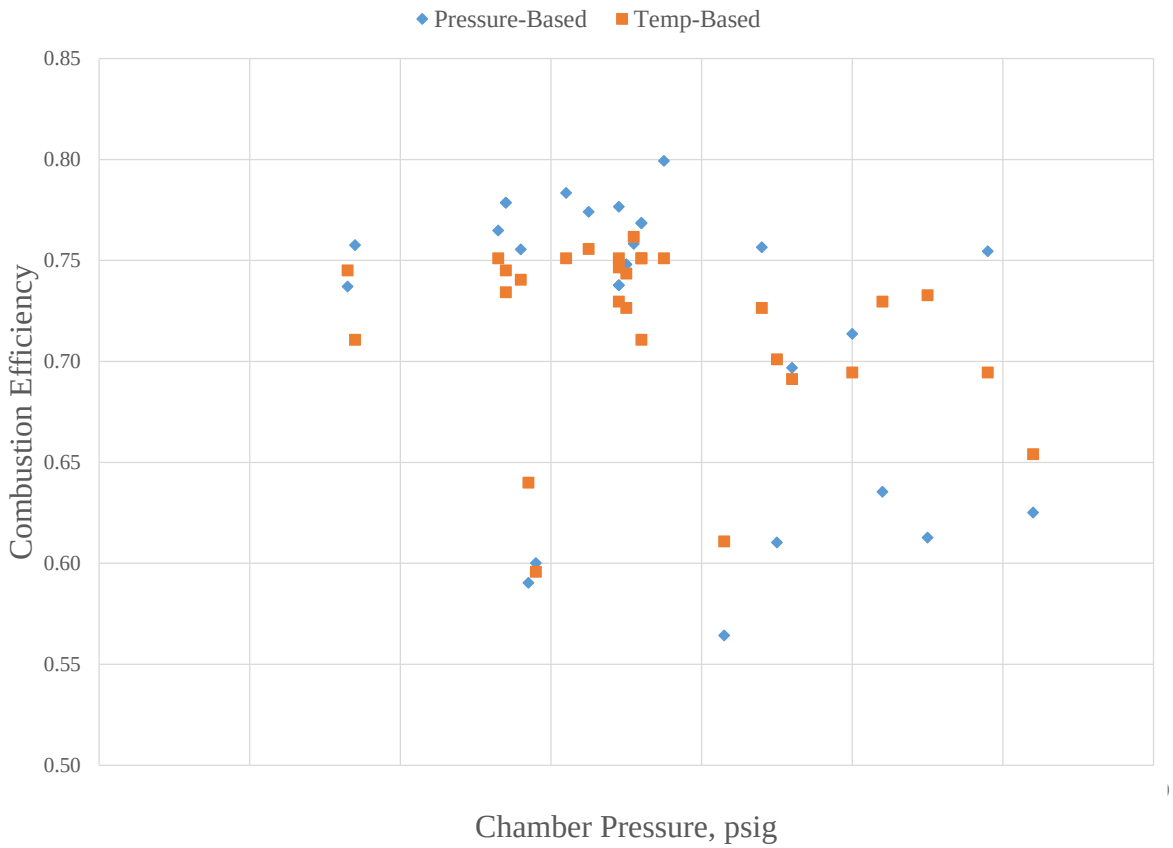

Figure 6.11. **Combustion efficiency vs chamber pressure**

while the temperature based calculated efficiencies are orange squares. Both the temperature based and pressure based efficiencies reside between 70 to 80 percent combustor efficiency with some outliers.

At pressures where the majority of testing took place, the pressure calculated efficiency and the temperature calculated efficiency are on average 3 percent of each other with some test pairs overlapping each other. As a general trend, the pressure based efficiencies show a slightly higher combustion efficiency within this range. At higher pressures, the trend appears to drop in the pressure calculated efficiency. This could be caused by small leaks in the instrumentation port fittings or in the nozzle assembly for tests with the volume reducing insert installed. This would have the effect of reducing the given chamber pressure of the test and thus reducing the calculated experimental characteristic velocity.

The same data are shown in Figure 6.12 but as a function of flow rate in mL/min. The pressure calculated and temperature calculated efficiencies show the trend of increasing efficiency at as flow rate increased. Once again there are a few outliers in the higher flow rate efficiencies showing three tests that only had 61 to 64 percent combustor efficiency. As stated previously, this could have been caused by improperly sealed instrumentation ports or nozzle piece which would have reduced the steady state chamber pressure obtained.

For low propellant flow rate tests of under 10 mL/min, the results obtained have shown underperformance of the workhorse system when compared to theory. One possible explanation for the cause of the lower chamber efficiency at the low flow rates could be due to the original design considerations of the workhorse thruster. Since the thruster was designed with a nominal

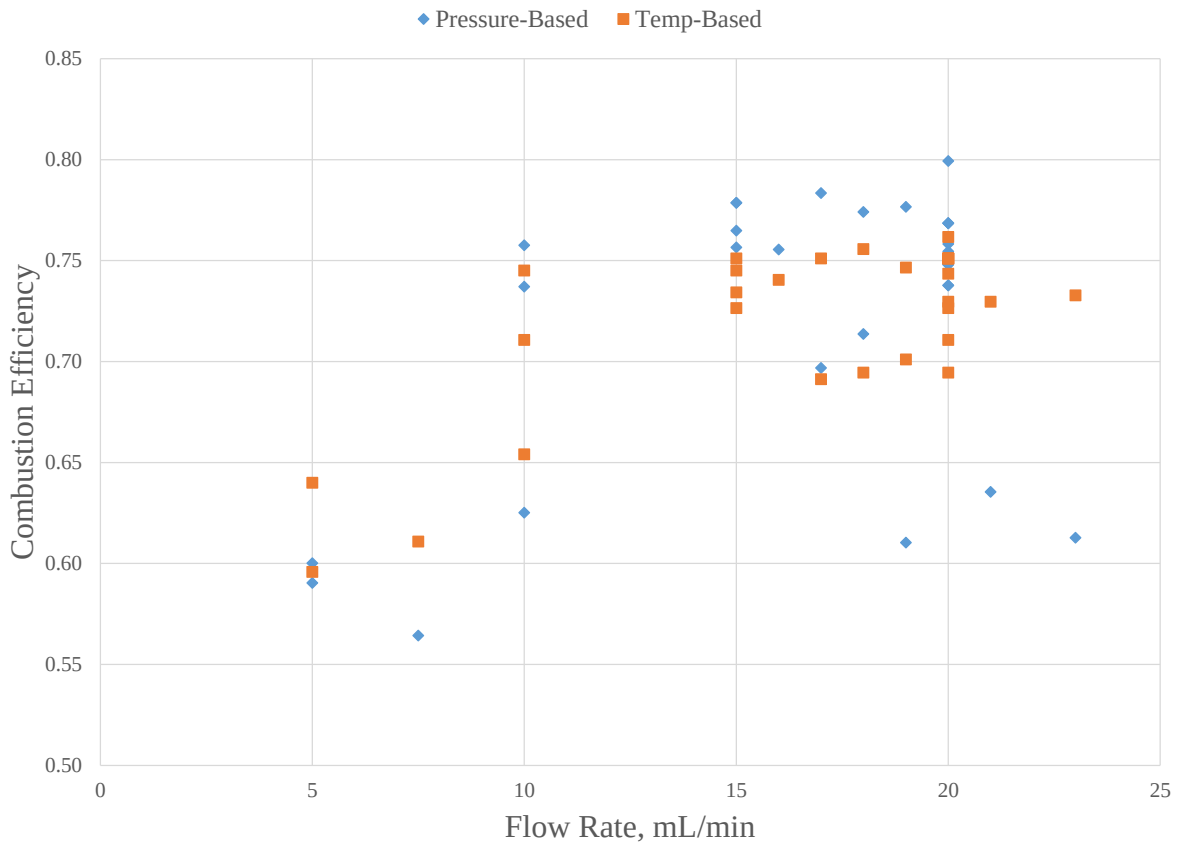

Figure 6.12. **Combustion efficiency vs propellant flow rate**

propellant flow rate of 20 mL/min in mind, when the flow rate is reduced the nozzle throat diameter must be smaller to maintain the same operating chamber pressure which causes the characteristic chamber length to become larger. The result is is the thermal mass and internal surface area per unit flow rate is increased to the point where heat transfer effects could play a considerable role at these lower flow rates.

Chapter 7. CONCLUSIONS

By utilizing a pressurized test cell, atomization characteristics and performance have been investigated for the injector technology used in a microthruster system using HAN-based monopropellant. In these tests, favorable results have been produced showing the capability of finely atomizing HAN-based monopropellant simulant.

In the flow-through reactor and open nozzle microthruster tests, the light off temperature of HAN-based monopropellant through a restricted environment has been established. By utilizing a see-through combustor design, the interaction between the atomized propellant and heated catalyst was observed and indicated a shorter length catalyst bed can be used for flow rates of interest. Tests with the see-through quartz combustor clearly showed that by finely atomizing the HAN-based monopropellant, a controlled reaction and burn can be initiated at preheat temperatures lower than that needed if the propellant was not fully atomized.

In workhorse microthruster hot fire tests conducted, the temperatures expected for complete combustion of HAN-based have not been definitively reached in the combustor. The combustion efficiency of the workhorse thruster was determined to be nominally 75 percent. Tests conducted with a volume reducing insert installed showed greater thruster responsiveness although at the cost of lower recorded temperatures in the catalyst bed and combustor region downstream of the catalyst. Pulsed operation testing showed that the monopropellant was reacting solely inside the catalyst bed with no post catalyst burning occurring. It was also found decomposition of HAN-based monopropellant may have a dependence on chamber pressure since there were no indications of propellant pooling on the catalyst in the workhorse thruster tests at flow rates where pooling was evident in the see-through quartz reactor tests.

REFERENCES

[1] Hawkins, T.W., Brand, A.J., McKay, M.B., Tinnirello, M., “Reduced Toxicity, High Performance Monopropellant at the U.S. Air Force Research Laboratory”, 4th International Association for the Advancement of Space Safety Conference, Huntsville, AL, 19-21 April 2010.

[2] Jankovsky, R.S., and Oleson, S.R., “HAN-Based Monopropellant Propulsion System with Applications”, NASA TM-107407, January 1997.

[3] Masse, R.K., Overly, J.A., Allen, M.Y., Spores, R.A., “A New State-of-the-Art in AF-M315E Thruster Technologies”, 48th AIAA/ASME/SAE/ASEE Joint Propulsion Conference & Exhibition, AIAA 2012-4335, Atlanta, GA, 30 July – 1 August 2012.

[4] Persson, M., Anflo, K., Dinardi, A., Bahu, J., "A Family of Thrusters for ADN-Based Monopropellant LMP-103S", 48th AIAA/ASME/SAE/ASEE Joint Propulsion Conference & Exhibit, AIAA 2012-3815, Atlanta, GA, 30 July – 1 August 2012.

[5] Sutton, G., and Biblarz, O., Rocket Propulsion Elements, 8th ed., John Wiley & Sons, Inc., New Jersey, 2010.

[6] Schmidt, E.W., “Hydroxylammonium nitrate compatibility tests with various materials – A Liquid Propellant Study”, Ft. Belvoir: Defense Technical Information Center, 1990. Print.

APPENDIX A: PROCEDURES

Hardware Setup

1. Obtain Propellant from locked cabinet on first floor.
2. Obtain Catalyst (locked cabinet) and HAN water bucket (fire cabinet) from Shockwave lab.
3. Decide if the chamber insert is to be used.
4. Decide on throat diameter for nozzle. If using the insert, put the nozzle in the insert using the thread sealant.
5. Decide which catalyst and which face is to be used.
6. Insert catalyst into bored-out end of the alumina sleeve. Use gloves to touch the catalyst and ensure nothing else touches it (grease, thread sealant, etc). This keeps the catalyst from becoming contaminated.
7. Put alumina spacer on top of catalyst.
8. Put wave washer on top of spacer.
   *Note, steps 6-8 are dependent on which alumina sleeve needed. If sleeves are changed, the order may change, and the wave washer may not be needed at all. The goal is to have alumina spacer or washer to be flush with the top of the sleeve.
9. Insert sleeve assembly into thruster body from the bottom, ensuring that the instrumentation holes in the sleeve align with those in the body.
10. Insert the upper temperature probes or put an allen wrench in the open instrumentation port to hold the sleeve in place for now.
11. Add a copper crush washer to the insert and add thread sealant to the threads. (Sealant not needed if the insert in step 13 is replaced)
12. Screw the insert in until it is tight. Ensure the instrumentation holes still line up. Note, if an allen wrench is used in step 10 to hold the sleeve in place, remove it before putting the insert in.
13. If the full combustor length is used and the insert is not wanted, remove the insert and screw in the threaded black nozzle. Put thread sealant on the threads before assembly. (The insert was used to make sure the crush washer was aligned properly.
14. Add thread sealant to the instrumentation plug's threads and assemble.
15. Insert remaining temperature probes and tighten down to appropriate level for Swagelok fittings. The proper placement is shown below.

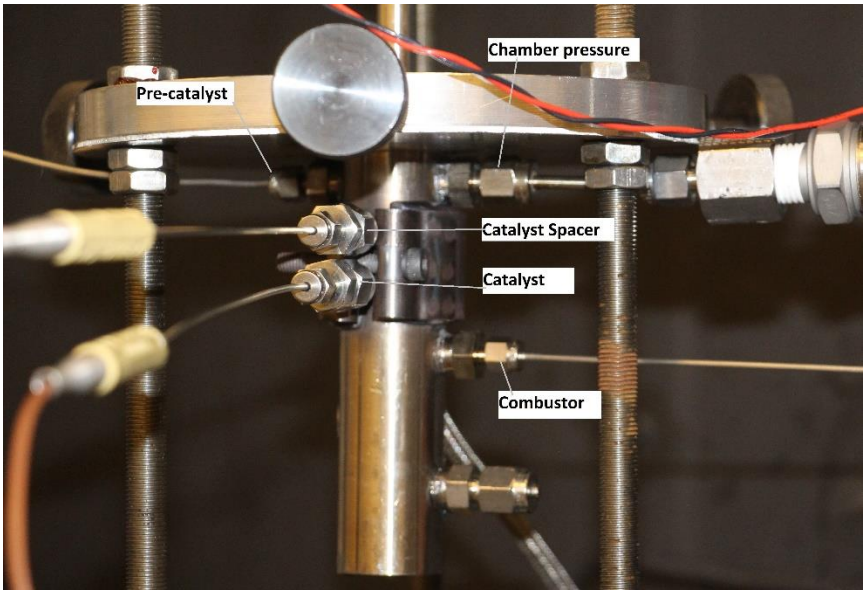

NOTE: If unclear which temperature sensor is which, load up the HAN_Control_Panel.vi, and start the data. Touch each thermocouple to see which one moves on the chart.

16. Connect Injector to the generator. Red to red… black to black.
17. Turn on the band heater.
18. Once the band heater has reached approximately 350° C, re-tighten either the insert or the black nozzle. These become loose as the thruster body heats up.

Software setup

1. Turn on Pump
2. Turn on power supply and verify it is set to 16V and 0.2A
3. Turn on Generator
4. Open HAN_Control_Panel_Vx.x.vi and run it. Probably will get the Power Interrupted message and need to restart the VI to get the pump connected
5. Configure generator software for current injector.
6. Create a new folder to house logs for the day's tests. Name it with the current date. Current location is under: C:\Users\microthruster\OneDrive\Documents\HAN\Testing\Microthruster\logs\Workhorse Thruster\Tests
7. Create an instrumentation file for the current test run and place it in the root of the test folder. Use the format of previous instrumentation files since data automation relies on that exact format.

Filling Procedures

NOTE: Use gloves when handling HAN. It's not as toxic as hydrazine, but it is an irritant.
NOTE: Always fill from clean propellant and push into used propellant. This prevents the clean propellant from being contaminated. (the exception is if you are intending to burn the used propellant.

1. Remove fill line from injector. The syringe can remain in the upright pump.
2. Withdraw 5ml from clean propellant bottle.
3. Push that 5ml into the used propellant bottle. This bleads the line to remove air.
4. If the propellant came out a little pink, repeat step 2-3.
5. Finally, withdraw 5ml, from the clean propellant bottle for testing.
6. Wipe off excess propellant from the tip of the line and attach the line to the injector.

Re- Filling Procedures

1. Use pump to withdraw 500 μL to prevent propellant from spilling out when disconnecting the line.
2. Disconnect line and inset into clean propellant.
3. Withdraw 5ml, from the clean propellant bottle for testing.
4. Wipe off excess propellant from the tip of the line and attach the line to the injector.

NOTE, there is now approx. 500 μL of dead volume in the injector. The next test should account for this dead volume.

DAQ Overview

This document describes the features of the Lab View program used to run HAN testing. Material here refers to version **2.1** of the program.
To launch the program, Open the Microthruster folder on the desktop (C:\Users\microthruster\Desktop\Microthruster) and click on the "DAQ" folder. Open the file named: "HAN_Control Panel v2.1.vi".
Click the White arrow in the upper left of the screen to run the program.

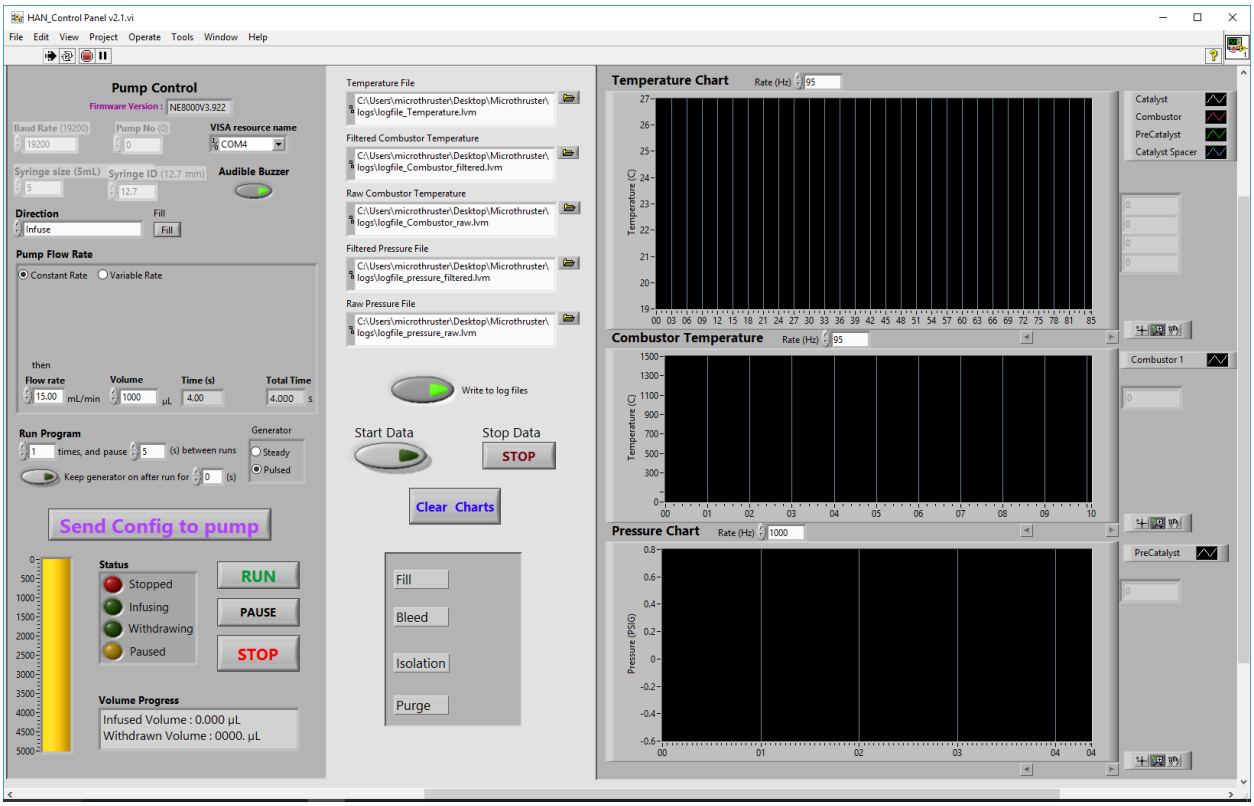
HAN_Control Panel v2.1.vi
File Edit View Project Operate Tools Window Help
Pump Control
Firmware Version : NE8000V3.922
Baud Rate (19200)
Pump No (0)
VISA resource name
COM4
Syringe size (5mL)
Syringe ID (12.7 mm)
Audible Buzzer
Direction
Infuse
Fill
Pump Flow Rate
Constant Rate
Variable Rate
then
Flow rate
15.00 mL/min
Volume
1000 µL
Time (s)
4.00
Total Time
4.000 s
Run Program
times, and pause
(s) between runs
Keep generator on after run for
(s)
Generator
Steady
Pulsed
Send Config to pump
Status
Stopped
Infusing
Withdrawing
Paused
RUN
PAUSE
STOP
Volume Progress
Infused Volume : 0.000 µL
Withdrawn Volume : 0000. µL
Temperature File
C:\Users\microthruster\Desktop\Microthruster\logs\logfile_Temperature.lvm
Filtered Combustor Temperature
C:\Users\microthruster\Desktop\Microthruster\logs\logfile_Combustor_filtered.lvm
Raw Combustor Temperature
C:\Users\microthruster\Desktop\Microthruster\logs\logfile_Combustor_raw.lvm
Filtered Pressure File
C:\Users\microthruster\Desktop\Microthruster\logs\logfile_pressure_filtered.lvm
Raw Pressure File
C:\Users\microthruster\Desktop\Microthruster\logs\logfile_pressure_raw.lvm
Write to log files
Start Data
Stop Data
STOP
Clear Charts
Fill
Bleed
Isolation
Purge
Temperature Chart
Rate (Hz) 95
Temperature (C)
Catalyst
Combustor
PreCatalyst
Catalyst Spacer
Combustor Temperature
Rate (Hz) 95
Combustor 1
Pressure Chart
Rate (Hz) 1000
Pressure (PSIG)
PreCatalyst

Pump Connection Section:

This section controls the connection to the syringe pump.

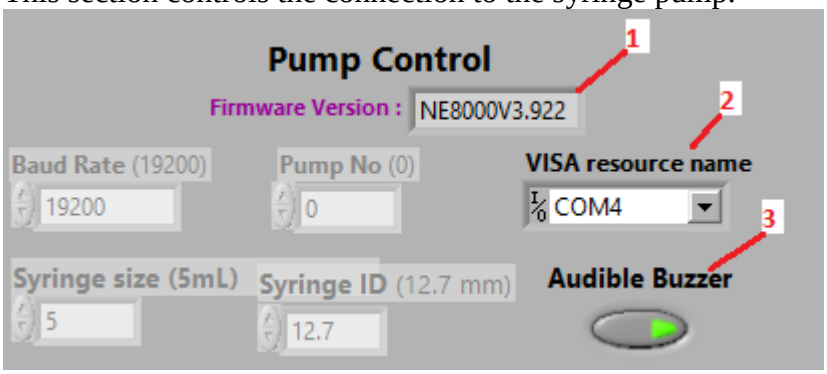

Most of the features here are read-only and don't need to be changed. Of note in this section are:

1. If this number is blank, the program is not connected to the pump. Make sure the pump is turned on. NOTE: The first time the program is run after the pump has been turned on, this number will be blank, and a popup saying "The power was interrupted" will display. If this happens, close the popup and restart the VI.
2. This is the COM port the pump is connected to on the local computer. If the pump is running and it can't connect, try changing this number
3. When this is lit, the pump will give audible beeps as feedback. One beep when commands are sent to the pump, and two beeps when the test completes.

Pump Operation Section:

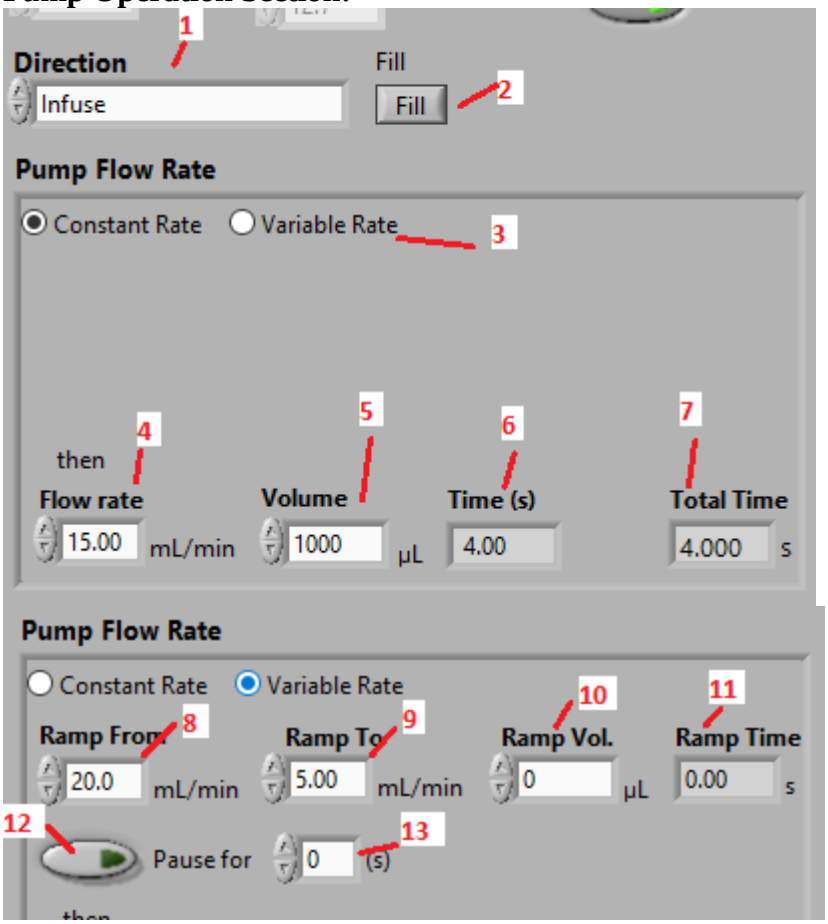

1. Sets whether the pump is infusing or withdrawing.
2. This is a macro that auto-sets the right numbers for filling the syringe. Not necessary, but is saves about 5 seconds each fill.
3. Sets the pump to operate at a constant or variable flow rate. Default is Constant since most tests are run like this.
4. Flow rate to pump at, in ml/min
5. Volume of propellant to dispense. Note, this must be entered in micro liters (µL).
6. Displays time the pumping will take with the current parameters.
7. Total pumping time. When in constant flow mode, this is the same as box 6. When in variable mode, it is the total of all operations.

When control 3 is set to Variable rate, these fields appear.

8. Starting flow rate to ramp from.
9. Ending flow rate to ramp to.
10. Total volume of propellant the flow rate should be ramped over.
11. Calculated time of the operation.
12. Optional switch to pause after the ramping operation.
13. If control 12 is selected, this is where you set the wait time.

Optional Pump Commands:

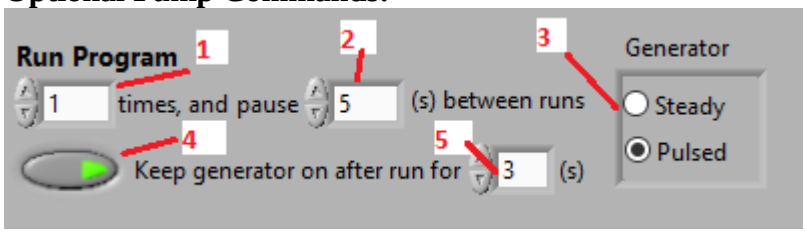

This section can be left as default if there is nothing fancy with your run.

1. If the pumping program is wanted to be run more than once, i.e. for a pulsed test, change this number.
2. Pause time between runs.
3. If doing more than 1 pulse (control 1 is > 1), this tells the generator whether to stay on constantly (“Steady”), or to turn off between pulses (“Pulsed).
4. Option to keep the generator on for a fixed time after the pumping has ended. The default is to stay on for 3 seconds to clear any remaining propellant from the injector face.
5. Number of seconds to keep generator on.

Run Program Section

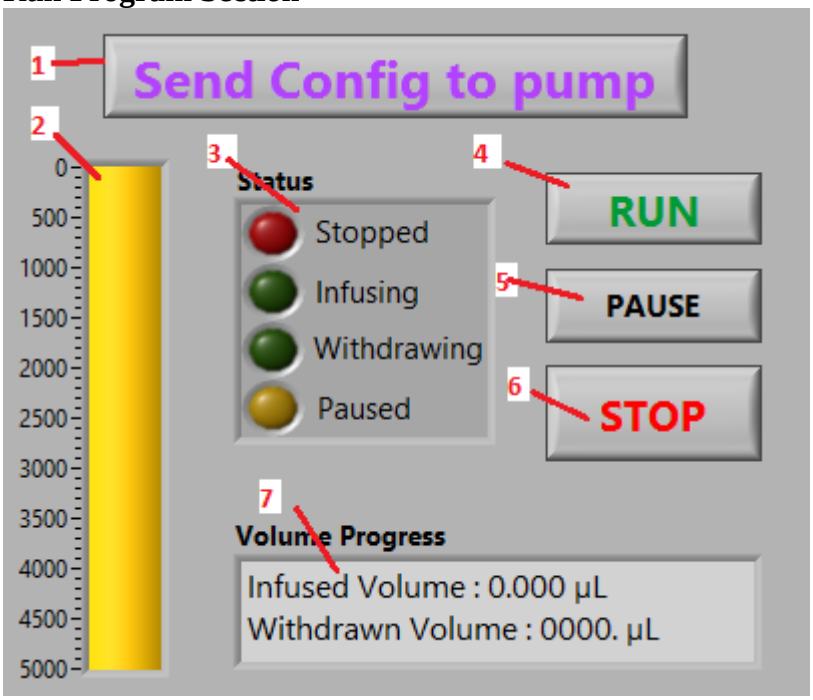

1. When all pump commands are set for the run, click this button to lock them in. This button must be clicked before the Run button will become operational. If a command needs to be changed after clicking this button, the VI will need to be stopped and restarted. Once the pump has completed its run. The pump commands can be edited again.
2. Indicator for amount of fluid remaining in the syringe. This resets every time the program starts and stops, so only useful if doing multiple runs on a single syringe.
3. Current pump status.
4. Run – This button executes the pumping /generator program. If the run has completed, but this button is still showing depressed, it is because the stops on the pump were hit before the total volume could be pumped. Click the stop button if this happens.
5. Pauses the run. Once paused, click the Run button (Control 4) to resume execution.
6. Stops the run at any point.
7. Displays the amount of fluid the pump infused or withdrew.

Data Control Section:

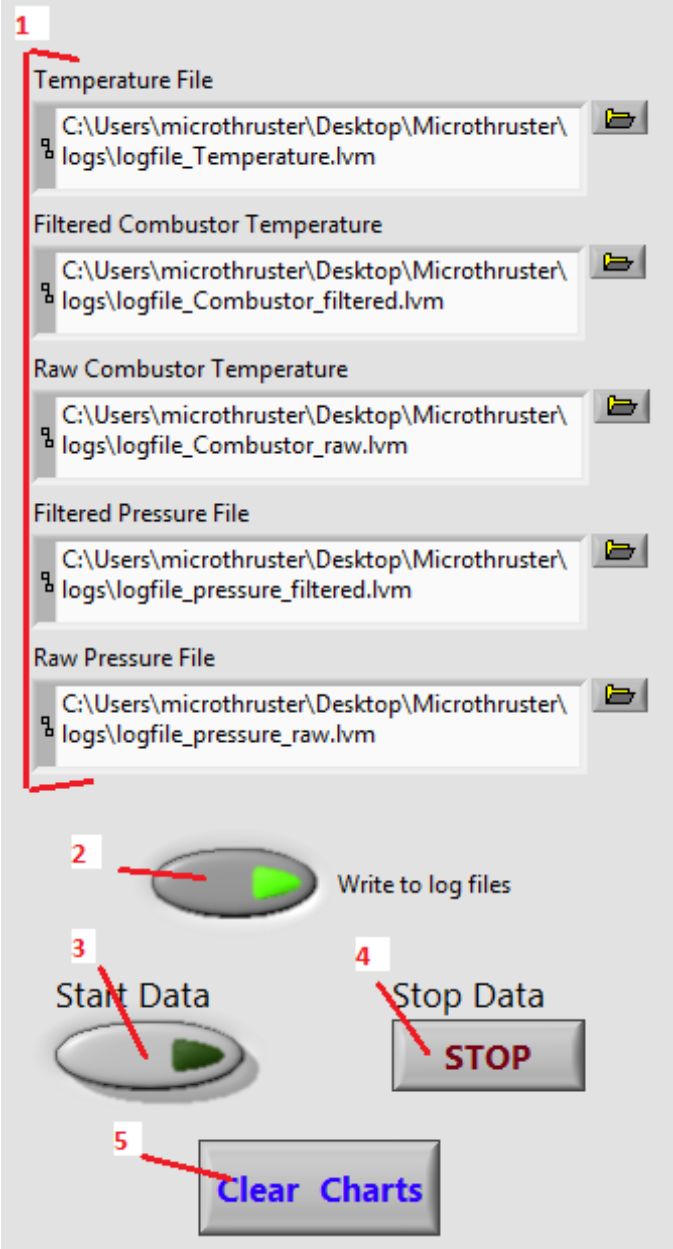

1. Optional section to change the path and/or filename of the log files. Can be left as default.
2. Turn off to disable writing to the log file. Useful when wanting to watch temperatures or pressures but don't care about saving the data.
3. Start data collection
4. Stop data collection
5. Clear the charts.

IMPORTANT: If the log files have been moved or deleted, the program needs to be restarted before attempting to write to log files again.

Data Chart Section:

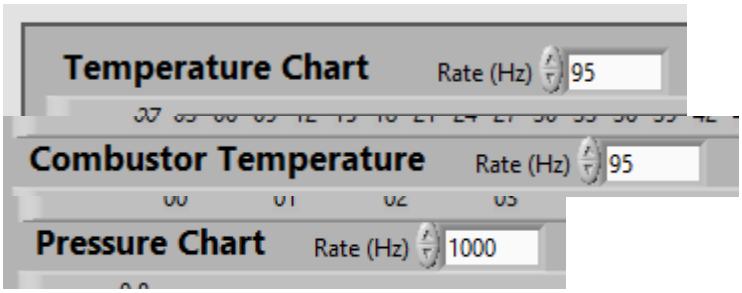

These three options are the only things configurable for the charts. Max Temperature rate for the type K chart (top one) is 95 Hz. If changing one of these numbers, VI needs to be restarted.

Hot-fire Checklist:

Before Test Run:

1. Verify Blast shield is in place and locked down with clamp.
2. Ensure syringe has enough propellant for test
3. Ensure all personnel have safety glasses on
4. Verify test parameters for the pump in the VI.
5. Ensure Generator software is set to correct numbers for test.
6. Ensure Write to Log Files button is selected.
7. Ensure Generator software has the start button highlighted.
8. Turn on Fume hood
9. Wait for catalyst to reach 400° C.
10. Click Send Command To Pump Button
11. Start Data
12. Click Run

After Test Run has Completed:

1. Stop Data
2. Move log files to archive location. Currently (C:\Users\microthruster\OneDrive\Documents\HAN\Testing\Microthruster\logs\Workhorse Thruster\Tests)
3. Restart VI since the logs were moved.
4. Turn off the Fume hood.

Hot-fire Cleanup:

IMPORTANT: Pretty much everything you do here is dealing with hot metal and ceramic. Pay attention at all times to what is being touched. Trust me.

1. Turn off band heater.
2. Turn off pump, generator, and power supply.
3. Remove the insert/black nozzle from the bottom of the thruster body. The best method to do this without touching the hot metal is to unscrew using the long end of the allen wrench and balance it on the end of the wrench to lay it down. Lay it down on the metal table to cool.

4. Remove the plug that is approx. 1.5” up from the bottom, on the left side of the thruster body.
   This guy:

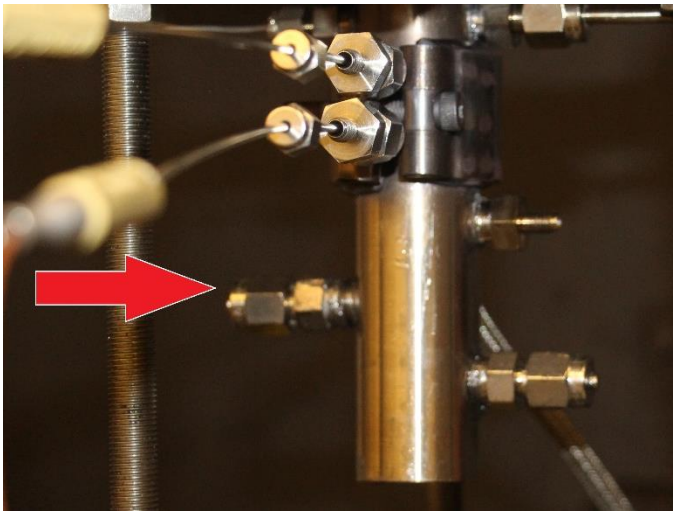

5. Insert a small allen wrench in the instrumentation hole that is uncovered. This will keep the sleeve from falling down prematurely.
6. Loosen and remove the Catalyst Spacer, Catalyst, and Combustor thermocouples.
7. Use the inserted allen wrench to gently push down on the alumina sleeve. This will pop out the copper crush washer. IMPORTANT: Don’t remove the allen wrench yet or the sleeve with fall down, shatter, and you are going to have a very bad day.
8. Find another allen wrench and stick the short end in the end of the sleeve. This wrench will support the sleeve.
9. Remove the upper allen wrench and let the bottom allen wrench support the sleeve. Work the sleeve down until you can fit the upper allen wrench back into the hole.
10. Use the two allen wrenches to maneuver the sleeve down to the table without touching it. (Again, it’s HOT). Always set the sleeve sideways to prevent it from falling over and breaking.
11. Once the sleeve is set down, use the wrenches to tip it up and slide the spacer and catalyst out.
12. Discard the used wave washer and copper crush washer.
13. Disconnect the syringe from the pump and flush the syringe and line with D.I. water.
    a. Insert line into di water and fill syringe.
    b. Move syringe around to ensure all sides get covered.
    c. Push water into HAN water bucket.
    d. Repeat a-c until the water comes out clear (approx. 3-4 times)
14. Flush the injector.
    a. Wait for the injector and thruster to fall below 100° C. Catalyst thermocouple may have to be pushed back in the body to get an accurate reading.
    b. Fill the syringe with D.I. water and push into injector. Catch the water with a beaker to be dumped into the HAN water bucket.
    c. Repeat step b until the water comes out clear. (approx. 2-3 times)

15. Fill syringe with air and push air out to get extra water out of line. Do this 4-5 times until water spray stops coming out.
16. Connect N_2 line to injector and blow 20-40 psi of N_2 into injector for 10 or so seconds to get rid of remaining water.
17. Clean out any container that held HAN water and dump into HAN water bucket.
18. Return Catalyst to its bag (again without touching the catalyst directly with your hands.)
19. Return Catalyst bag, propellant, and HAN water bucket to their respective storage places.

APPENDIX B: DRAWINGS

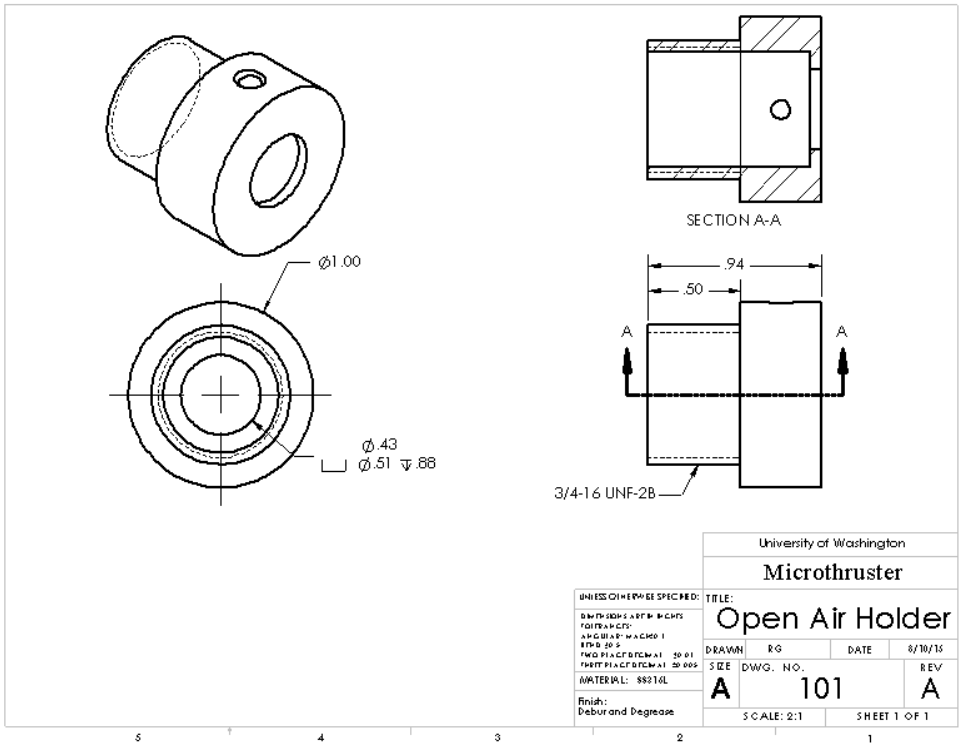

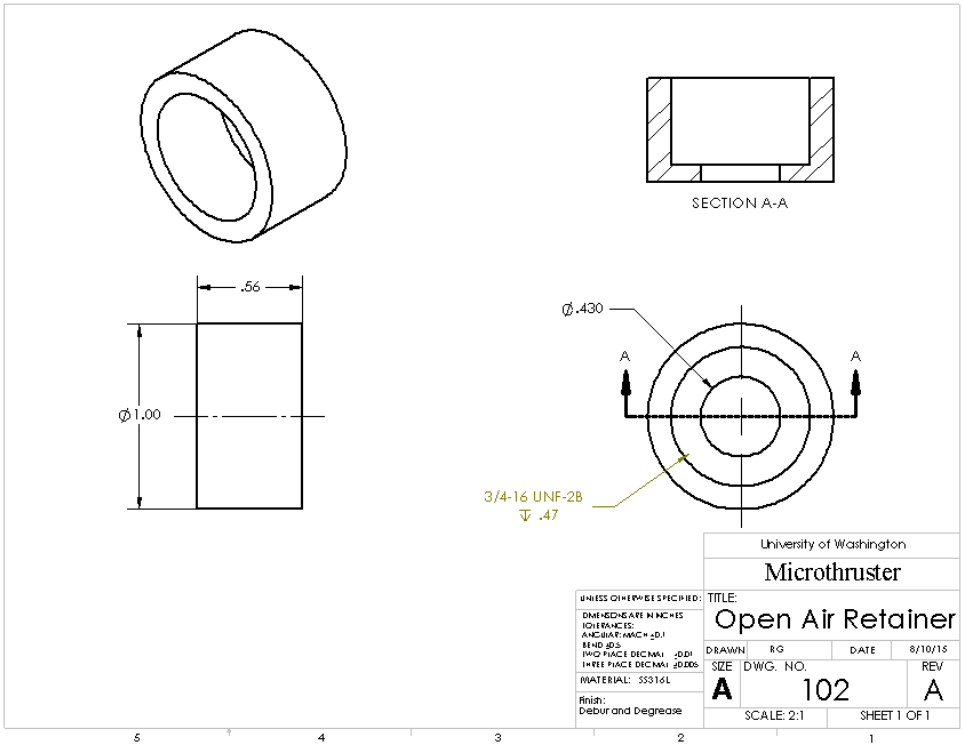

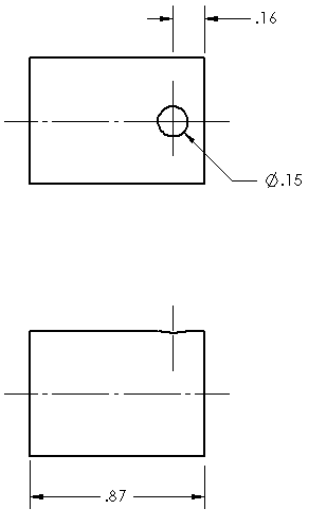

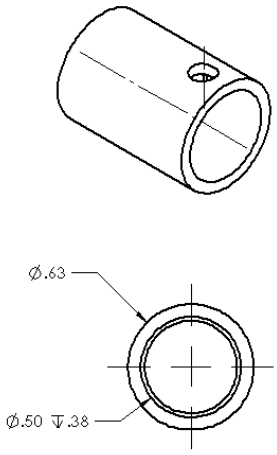

University of Washington	
Microthruster	
UNLESS OTHERWISE SPECIFIED: DIMENSIONS ARE IN INCHES TOLERANCES: ANGULAR: MACH ±0.1 BEND ±0.5 TWO PLACE DECIMAL ±0.01 THREE PLACE DECIMAL ±0.005 MATERIAL: Alumina Finish:	TITLE: Alumina Sleeve
DRAWN RG	DATE 1/26/16
SIZE A	DWG. NO. 101 REV A
SCALE: 2:1	WEIGHT: 0.02 SHEET 1 OF 1

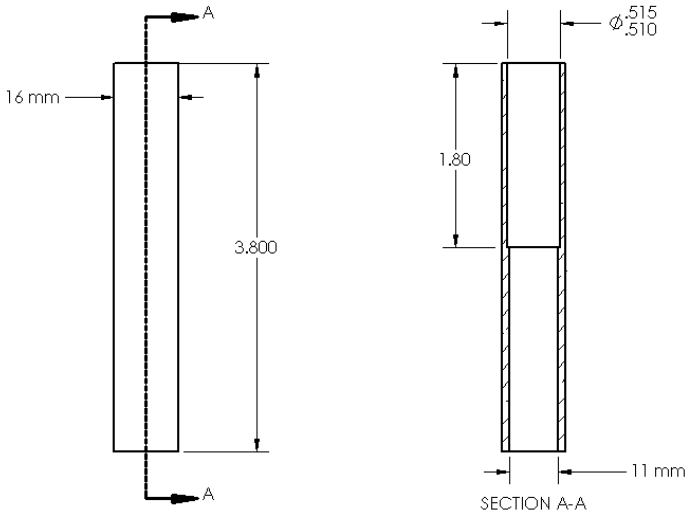

University of Washington	
Microthruster	
UNLESS OTHERWISE SPECIFIED: DIMENSIONS ARE IN INCHES TOLERANCES: ANGULAR: MACH ±0.1 BEND ±0.5 TWO PLACE DECIMAL ±0.01 THREE PLACE DECIMAL ±0.005 MATERIAL: Quartz Finish:	TITLE: Quartz Combustor
DRAWN RG	DATE 8/1/16
SIZE A	DWG. NO. 110 REV A
SCALE: 1:1	WEIGHT: 0.04 SHEET 1 OF 1

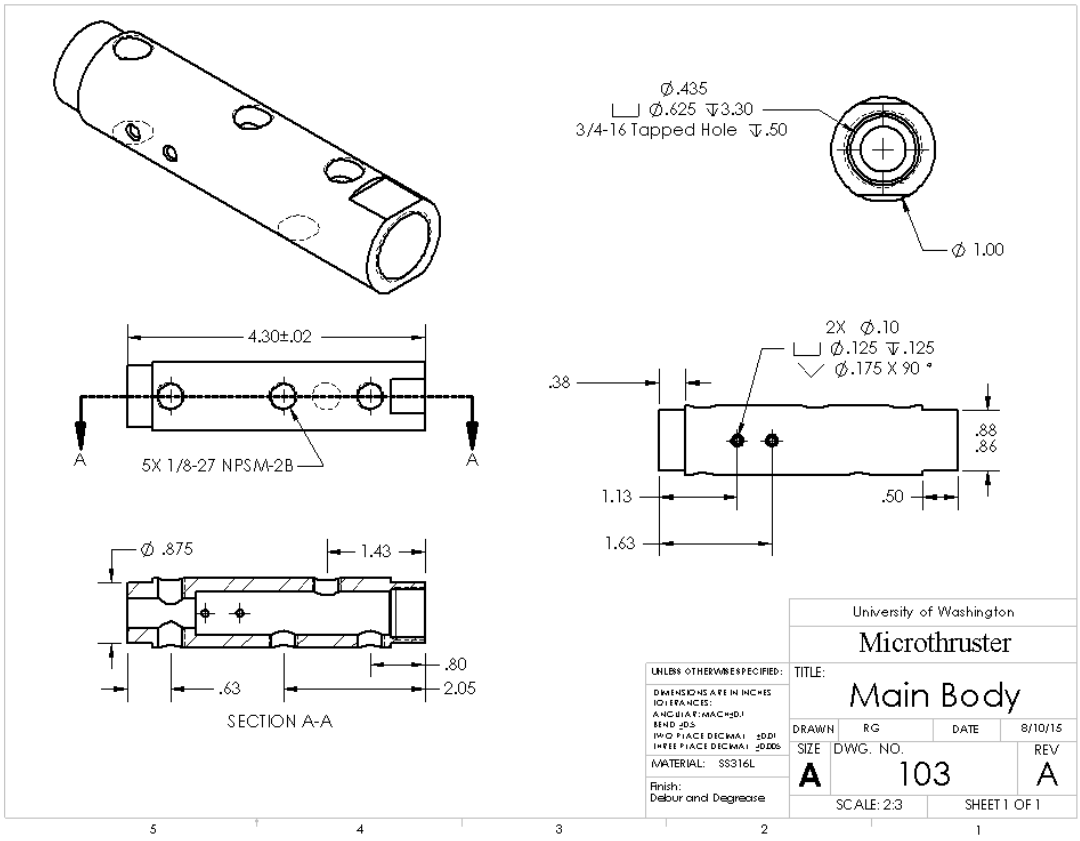
Ø.435
⌴ Ø.625 ↧3.30
3/4-16 Tapped Hole ↧.50
Ø 1.00
4.30±.02
A
A
5X 1/8-27 NPSM-2B
2X Ø.10
⌴ Ø.125 ↧.125
Ø.175 X 90 °
.38
.88
.86
1.13
.50
1.63
Ø .875
1.43
.80
.63
2.05
SECTION A-A
University of Washington
Microthruster
UNLESS OTHERWISE SPECIFIED:
DIMENSIONS ARE IN INCHES
TOLERANCES:
ANGULAR: MACH ±0.1
BEND ±0.5
TWO PLACE DECIMAL ±0.01
THREE PLACE DECIMAL ±0.005
MATERIAL: SS316L
Finish:
Deburr and Degrease
TITLE:
Main Body
DRAWN RG DATE 8/10/15
SIZE A
DWG. NO. 103
REV A
SCALE: 2:3
SHEET 1 OF 1
5 4 3 2 1

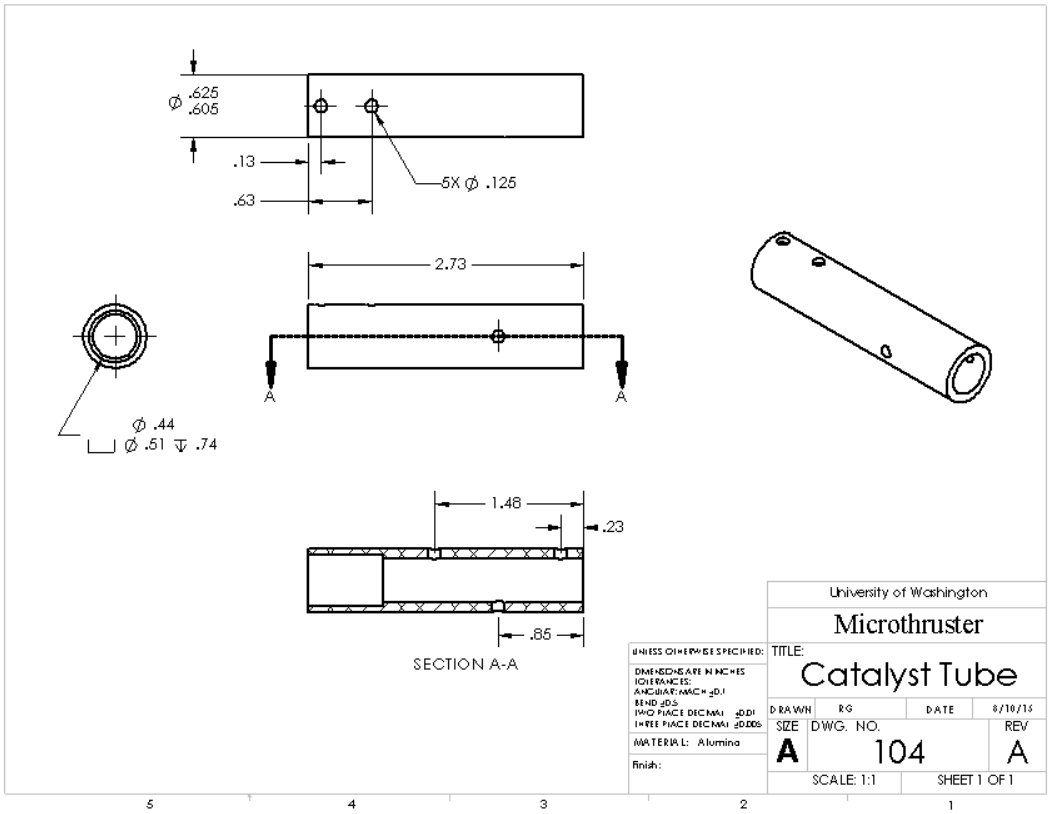
Ø .625
Ø .605
.13
.63
5X Ø .125
2.73
A
A
Ø .44
⌴ Ø .51 ↧ .74
1.48
.23
.85
SECTION A-A
University of Washington
Microthruster
UNLESS OTHERWISE SPECIFIED:
DIMENSIONS ARE IN INCHES
TOLERANCES:
ANGULAR: MACH ±0.1
BEND ±0.5
TWO PLACE DECIMAL ±0.01
THREE PLACE DECIMAL ±0.005
MATERIAL: Alumina
Finish:
TITLE:
Catalyst Tube
DRAWN RG DATE 8/10/15
SIZE A
DWG. NO. 104
REV A
SCALE: 1:1
SHEET 1 OF 1
5 4 3 2 1

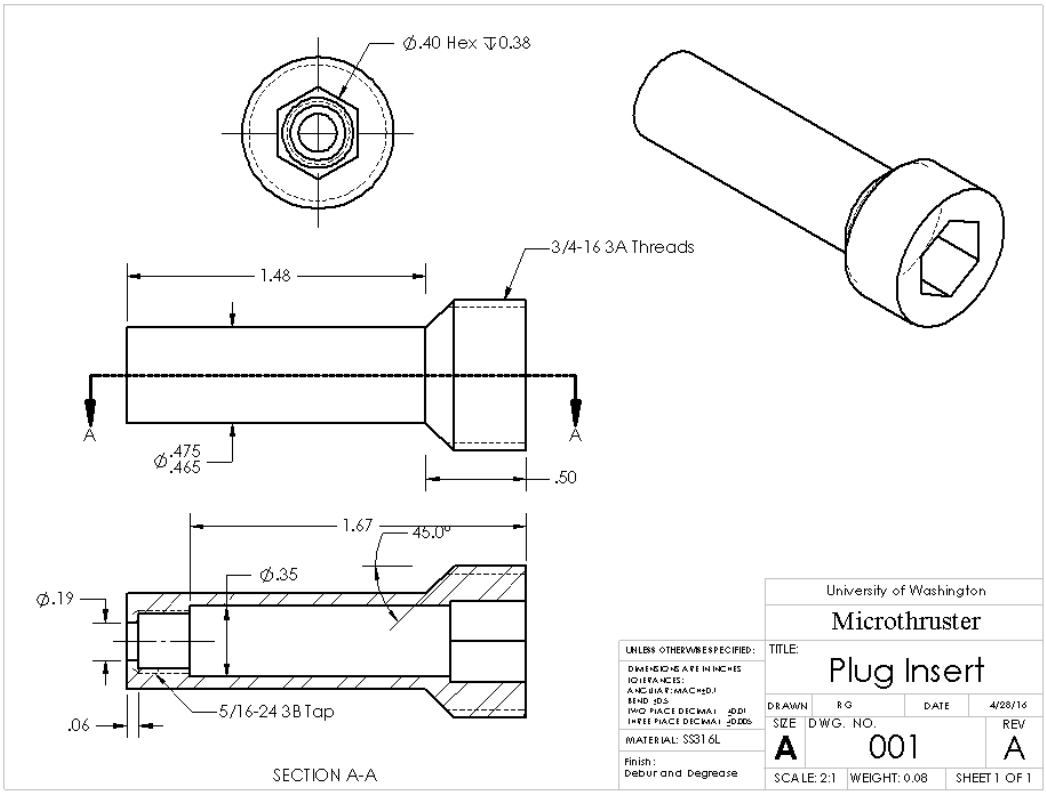
Ø.40 Hex ↧0.38
3/4-16 3A Threads
1.48
A
A
Ø.475
Ø.465
.50
1.67
45.0°
Ø.35
Ø.19
.06
5/16-24 3B Tap
SECTION A-A
University of Washington
Microthruster
UNLESS OTHERWISE SPECIFIED:
DIMENSIONS ARE IN INCHES
TOLERANCES:
ANGULAR: MACH ±0.1
BEND ±0.5
TWO PLACE DECIMAL ±0.01
THREE PLACE DECIMAL ±0.005
MATERIAL: SS316L
Finish:
Debur and Degrease
TITLE:
Plug Insert
DRAWN RG
DATE 4/28/16
SIZE A
DWG. NO. 001
REV A
SCALE: 2:1
WEIGHT: 0.08
SHEET 1 OF 1

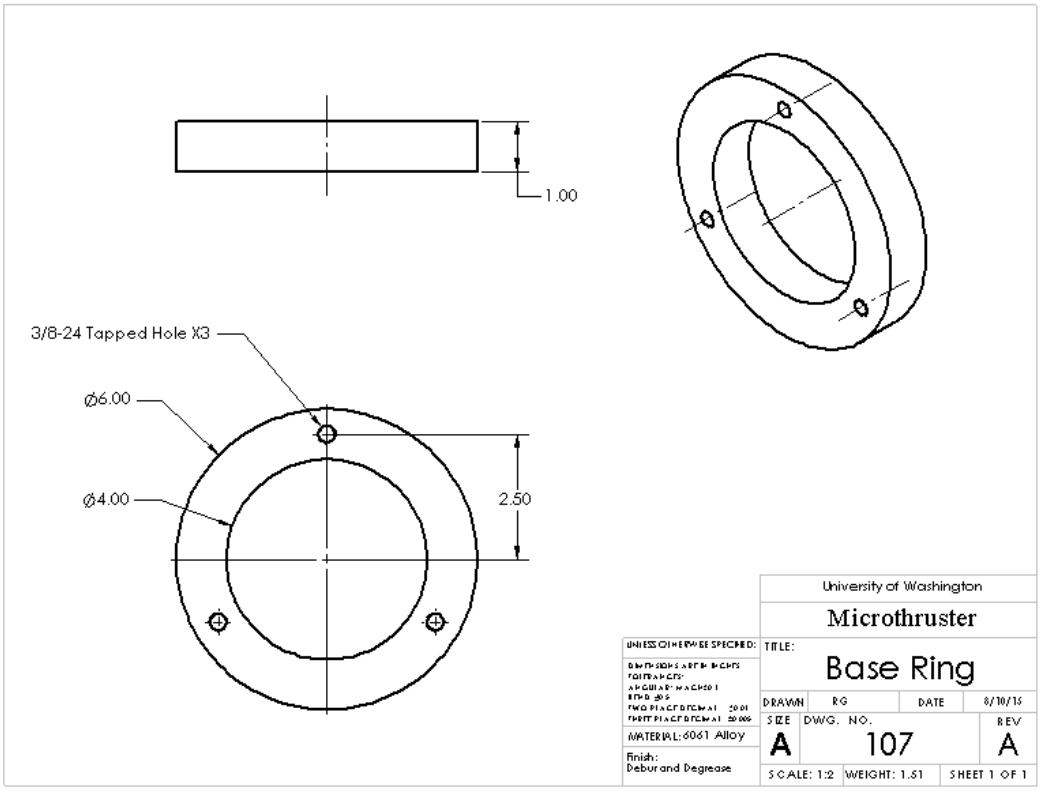
1.00
3/8-24 Tapped Hole X3
Ø6.00
Ø4.00
2.50
University of Washington
Microthruster
UNLESS OTHERWISE SPECIFIED:
DIMENSIONS ARE IN INCHES
TOLERANCES:
ANGULAR: MACH ±0.1
BEND ±0.5
TWO PLACE DECIMAL ±0.01
THREE PLACE DECIMAL ±0.005
MATERIAL: 6061 Alloy
Finish:
Debur and Degrease
TITLE:
Base Ring
DRAWN RG
DATE 8/10/16
SIZE A
DWG. NO. 107
REV A
SCALE: 1:2
WEIGHT: 1.51
SHEET 1 OF 1

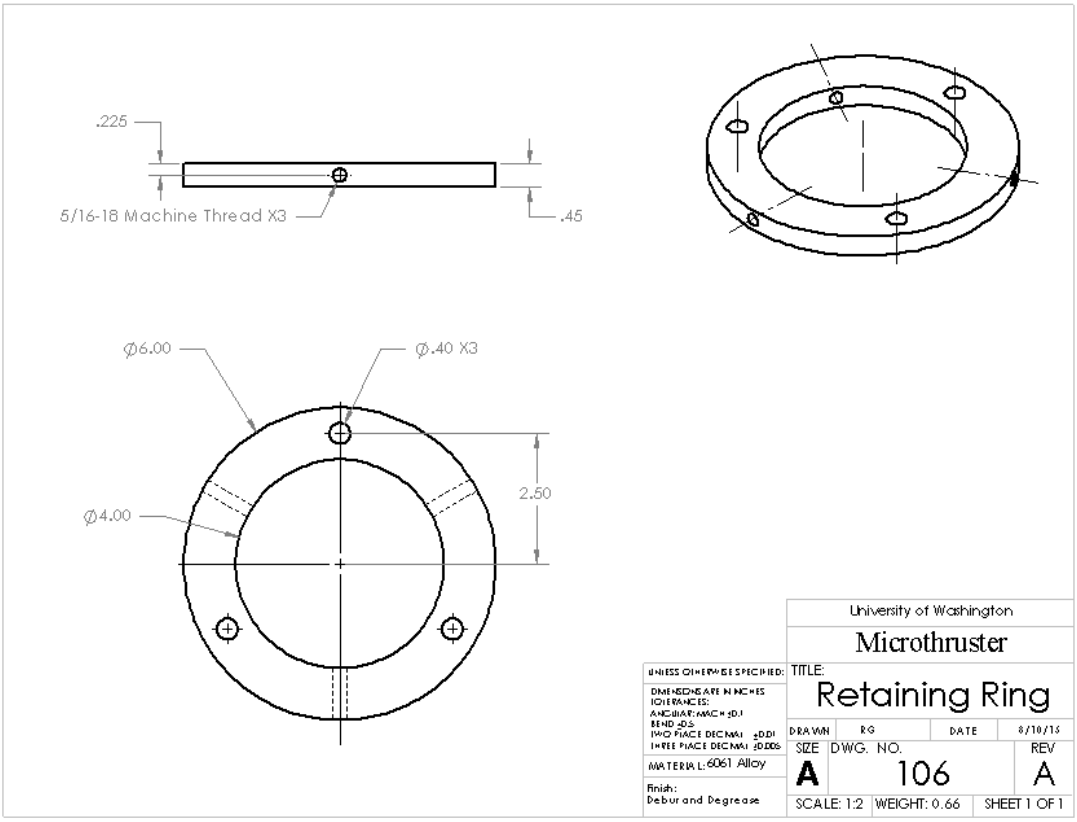

UNLESS OTHERWISE SPECIFIED:	University of Washington
DIMENSIONS ARE IN INCHES TOLERANCES: ANGULAR: MACH ±0.1 BEND ±0.5 TWO PLACE DECIMAL ±0.01 THREE PLACE DECIMAL ±0.005	Microthruster TITLE: Retaining Ring
MATERIAL: 6061 Alloy	DRAWN RG DATE 8/10/15
Finish: Debur and Degrease	SIZE A DWG. NO. 106 REV A
	SCALE: 1:2 WEIGHT: 0.66 SHEET 1 OF 1

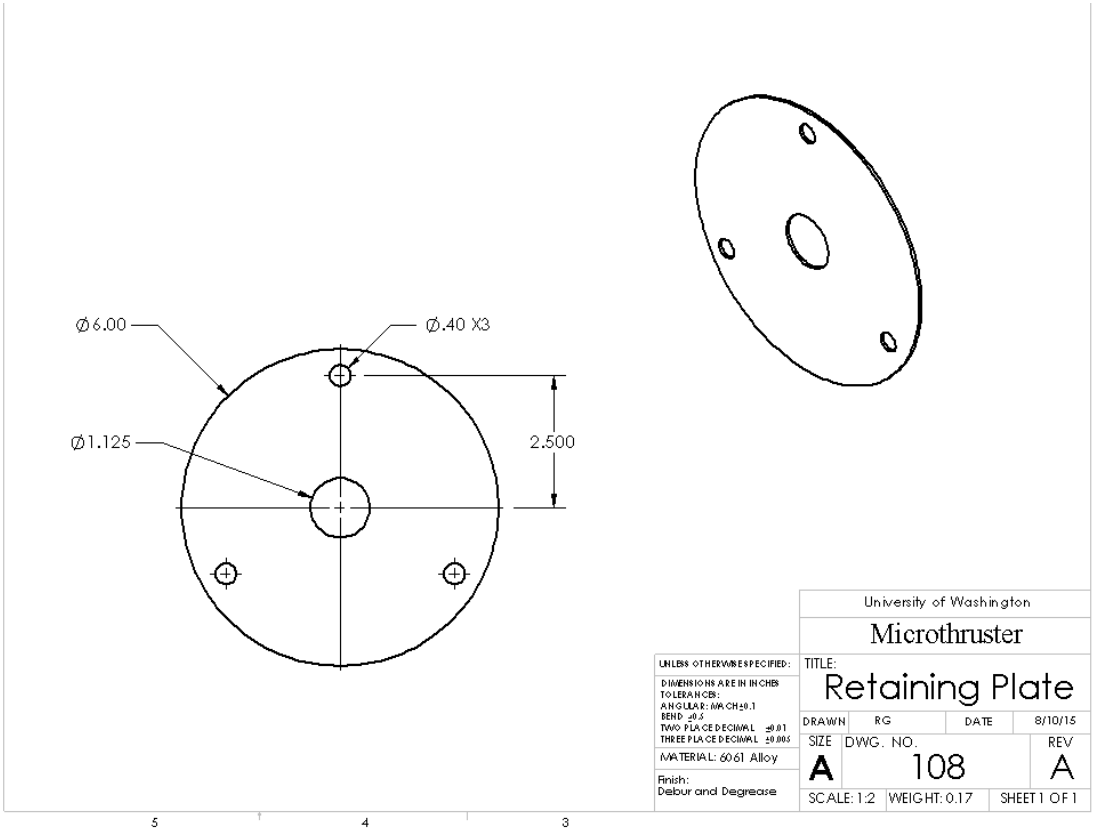

UNLESS OTHERWISE SPECIFIED:	University of Washington
DIMENSIONS ARE IN INCHES TOLERANCES: ANGULAR: MACH ±0.1 BEND ±0.5 TWO PLACE DECIMAL ±0.01 THREE PLACE DECIMAL ±0.005	Microthruster TITLE: Retaining Plate
MATERIAL: 6061 Alloy	DRAWN RG DATE 8/10/15
Finish: Debur and Degrease	SIZE A DWG. NO. 108 REV A
	SCALE: 1:2 WEIGHT: 0.17 SHEET 1 OF 1

APPENDIX C: MATLAB DATA EXTRACT CODE

```
clear all; close all; clc;
%%%%%%%%%%%%%%%%%%%%%%%%%%%%%%%%%%%%%%%%%%%%%%%%%%%%%%%%%%%%%%%%%%%%%%%%%%%%%%
%%%%%%%%%
%% User Inputs
%%%%%%%%%%%%%%%%%%%%%%%%%%%%%%%%%%%%%%%%%%%%%%%%%%%%%%%%%%%%%%%%%%%%%%%%%%%%%%
%%%%%%%%%
instFileDir =  '\';  %Directory of Instrumentation file location, including
trailing '\'  ex: 'd:\logs\'
instFile = 'Instrumentation.xlsx';

logFileDir = '\';  %Directory of Log File location, including trailing '\'
%If no typeC thermocouple, you can ignore the filename1, ch1, and plot1
inputs.

filename1 = 'logfile_Combustor_filtered.lvm'; %type c
ch1=2; %number of channels + time
plot1=2; %number of channels to plot + time
filename2 = 'logfile_pressure_filtered.lvm'; %pressure
ch2=2; %number of channels + time
plot2=2; %number of channels to plot + time
filename3 = 'logfile_Temperature.lvm'; %type k
ch3=5; %number of channels + time
plot3=3; %number of channels to plot + time

%timestamp to start and end graph. Both values must be a number
timeStart = 0;
timeEnd = 80;
%Pressure levels to start and end graph. Defaults are 0 to inf
pressureStart = 0;
pressureEnd = inf;
%Temperature levels to start and end graph. Defaults are 300 to inf
temperatureStart = 300;
temperatureEnd = inf;
%%%%%%%%%%%%%%%%%%%%%%%%%%%%%%%%%%%%%%%%%%%%%%%%%%%%%%%%%%%%%%%%%%%%%%%%%%%%%%
%%%%%%%%%
%% NO NEED TO CHANGE ANYTHING BELOW HERE :)

%read in the instrumentation file to get names of channels
[channelNums,channelTxt] = xlsread([instFileDir,instFile],'Sheet1','A6:D13'
);

%only run typeC code if the channel is defined
typeC = ~strcmp(channelTxt(1,2),'');
if typeC==0 %clear out bogus input data
   filename1='';
   ch1=0;
   plot1=0;
end

%pull legend titles from instrumentation file
legTitles = [channelTxt(:,1);channelTxt(:,2);channelTxt(:,3)];
legTitles(strcmp(legTitles,'')) = [];
```

```
%% Data procurement from LABview output file and Instrumentation Log
%creates color scheme of most diverse colors
%count=ch1+ch2+ch3;
colors=distinguishable_colors(7); %hardcode numbers so they are always the
same
colors(4,:)=[]; colors(6,:)=[];

if typeC == 1
    fid = fopen([logFileDir,filename1]);
    %A = textscan(fid,'%f','headerlines',22,'delimiter',',');
    A = textscan(fid,'%f','delimiter',',');
    check=length(A{1})/ch1;
    big_data1=reshape(A{1},ch1,check)';
    fclose(fid);
end

%Pressure
fid = fopen([logFileDir,filename2]);
%A = textscan(fid,'%f','headerlines',23,'delimiter',',');
A = textscan(fid,'%f','delimiter',',');
check=length(A{1})/ch2;
big_data2=reshape(A{1},ch2,check)';
fclose(fid);

%Type-K Temperature
fid = fopen([logFileDir,filename3]);
%A = textscan(fid,'%f','headerlines',25,'delimiter',',');
A = textscan(fid,'%f','delimiter',',');
check=length(A{1})/ch3;
big_data3=reshape(A{1},ch3,check)';
fclose(fid);

if typeC == 1;
    time1=big_data1(:,1);
end
time2=big_data2(:,1);
time3=big_data3(:,1);

f=figure();

hold on
count = 1;
cc = 1; %colorcount
for jj=2:plot3
    leg(count)=plot(time3,big_data3(:,jj),'Color',colors(cc,:),'LineWidth',
2);
    count=count+1;
    cc = cc+1;
end
if typeC == 1
    for j=2:plot1
        leg(count)=plot(time1,big_data1(:,j),'Color',colors(end,:));
        count=count+1;
    end
```

```
end
hold off;
xlabel('Time, s')
ylabel('Temperature, ^{\circ}C')

ax1=gca;
ax1.XAxis.Visible = 'off';

ax2= axes('Position',get(ax1,'Position'),...
       'XAxisLocation','bottom',...
       'YAxisLocation','right',...
       'Color','none',...
       'XColor','k','YColor','k');
linkaxes([ax1 ax2],'x');

hold on;
%'leg' var keeps track of inidvidual line handles for the combined legend
call
for jjj=2:plot2

leg(count)=plot(time2,big_data2(:,jjj),'Color','k','Parent',ax2);%,'LineWidth
',2);
    count=count+1;
end
hold off;

%set the post-plot graph limits
ax1.YGrid = 'on';
ax1.YMinorTick = 'on';
ylim(ax1,[temperatureStart,temperatureEnd]);
ax2.XMinorTick = 'on';
ax2.YMinorTick = 'on';
xlim(ax2,[timeStart,timeEnd]);
ylim(ax2,[pressureStart,pressureEnd]);
set(ax2,'Xtick',timeStart:5:timeEnd);


%Define the legend values
if typeC == 1
%    legend([leg],{'Combustor','Catalyst','Pre-Catalyst Chamber','Catalyst
Spacer','Chamber Pressure'},'Location','NorthEast');
    legend([leg],legTitles,'Location','NorthEast');
else
   legend([leg],{'Catalyst','Combustor','Chamber
Pressure'},'Location','NorthEast');%'Pre-Catalyst Chamber','Catalyst
Spacer','Chamber Pressure'},'Location','NorthEast');
%     legend([leg],legTitles,'Location','NorthEast');
end
%title(figureTitle);
ylabel('Pressure, PSIG')
xlabel('Time, s')
```

APPENDIX D: MATLAB FFT CODE

```
clear all; close all; clc;

logFileDir = '\';  %Directory of Log File location, including trailing '\'
filename2 = 'logfile_pressure_raw.lvm'; %pressure
ch2=2; %number of channels + time

%Read in Pressure File
fid = fopen([logFileDir,filename2]);
%A = textscan(fid,'%f','headerlines',23,'delimiter',',');
A = textscan(fid,'%f','delimiter',',');
check=length(A{1})/ch2;
big_data2=reshape(A{1},ch2,check)';
fclose(fid);

%Truncate Pressure Data...Useful with pressure gradient
d=big_data2(13000:18000,:);
% plot(v(:,2))
% xlabel('Time [sec]');
% ylabel('Amplitude');
% title('Signal of Interest, v(n)');

tf=d(:,1);
t=tf(:)-tf(1);
L=tf(end)-d(1,1);
d=d(1:end-1,2);
t=t(1:end-1);
t=reshape(t,1,length(t));

%subtracts mean value of number of sections, depends on pressure gradient
nsect=5;
lsect=length(d)/nsect;
vn=[];
for jj=0:nsect-1
    startsect=jj*lsect+1;
    endsect=startsect+lsect-1;
    vsect=d(startsect:endsect);
    vsects=vsect-mean(vsect);
    vn=[vn; vsects];
end

v=vn/max(abs(vn));
n=length(v); %same number of points as in data

v=reshape(v,1,n);
t=reshape(t,1,n);
k=(1/(2*L))*[0:n/2-1 -n/2:-1];

ks=fftshift(k);
vt=fft(v);

%% Preview of Size of Wavelet
% width=25;
```

```
% g=exp(-width*(t-2).^2);
% gm=2/((3*width).^(1/2).*pi.^(1/4))*(1-(t-2).^2/width.^2).*exp(-(t-
2).^2/(2*width.^2));
% plot(t,v,'b',t,g,'g')
% title('Wavelet')

%% Gaussian Wavelet

n=0; %used for counter for the subplot
dt=[.05]; %time step
width=[50]; %gaussian width, larger number is smaller width
spec=[];
for jjj=1:length(width);
    for tt=1:length(dt)
    tslide=0:dt(tt):9;
        for jj=1:length(tslide)

        g=exp(-width(jjj)*(t-tslide(jj)).^2);
        vg=g.*v;
        vgt=fft(vg);

        spec=[spec; abs(fftshift(vgt))/max(abs(vgt))];
        end

        n=n+1;
%     figure
    subplot(length(width),length(dt),n),
    pcolor(tslide,ks,spec.'),shading interp
    axis([0 5 0 50])
    xlabel('Time (S)');
    ylabel('Frequency (Hz)');
    title(['Dt=' num2str(dt(tt)) ', Width=' num2str(width(jjj))]);
    %saveas(gcf,['dt=' num2str(dt(tt)) ' Filter Width='
num2str(width(jjj))],'png');

subplot(3,1,1), plot(t,v)
xlabel('Time, s')
ylabel('Amplitude')
subplot(3,1,2), plot(ks,abs(fftshift(vt))/max(abs(vt)))
axis([0 100 0 1])
xlabel('Frequency, Hz')
ylabel('Amplitude')
subplot(3,1,3),
pcolor(tslide,ks,spec.'),shading interp
axis([0 t(end)+.001 0 50])
xlabel('Time, s');
ylabel('Frequency, Hz');

    spec=[];
    end
end
```